Examining Parkinson's disease linked DJ-1 and its interaction with autophagy related ATG5 and ATG12 & Understanding PINK1's functional interaction with mitochondrial m-AAA protease AFG3L2

By Matthew Alexander Seegobin

This thesis is submitted to the Faculty of Graduate and Postdoctoral Studies as a partial fulfillment of the requirements for the M.Sc. program in Neuroscience

Faculty of Medicine
Dept. of Cellular and Molecular Medicine
University of Ottawa

ABSTRACT:

Mutations in DJ-1 and PTEN-induced putative kinase 1 (PINK1) have been linked to familial early-onset Parkinson's disease. However, their functional role is not well understood. Through a mass-spectrometry screen we identified protein interaction candidates ATG5 and ATG12 for DJ-1 and AFG3-like AAA ATPase 2 (AFG3L2) for PINK1. Examination of ATG5, ATG12, and DJ-1 by co-immunoprecipitation through multiple methods, did not validate the interaction. In contrast, the interaction between m-AAA protease AFG3L2 and PINK1 was validated. AFG3L2 selectively stabilized and can differentially cleave PINK1 *in-vitro*. We observed endogenous mitophagy in AFG3L2 null cells. Furthermore, we elucidated a novel function of mitochondrially-targeted PINK1 fragments in rescuing endogenous mitochondrial fragmentation, increasing both mitochondrial length and networking. Although further examination is needed, these studies provide a greater understanding of the functional interaction between PINK1 and AFG3L2 and provide evidence that DJ-1, ATG5 and ATG12 may not interact.

TABLE OF CONTENTS

LIST OF FIGURES

LIST OF ABBREVIATIONS

AAA	ATPase associated with diverse cellular activities
aa	Amino acid
AFG3L2	AFG3-like AAA ATPase 2
ATG	Autophagy Related
ATG8-PE	ATG8- Phosphatidylethanolamine
ATP	Adenosine triphosphate
CCCP	Carbonyl Cyanide m-Chlorophenylhydrazone
CI	Complex I
CMA	Chaperone mediated autophagy
CO_2	Carbon Dioxide
CV	Complex V
DIV	Days *in vitro*
DMEM	Dulbeccos's modified eagle's medium
DNA	Deoxyribonucleic acid
EBSS	Earls balanced salt solution
FBS	Fetal bovine serum
GFP	Green florescent protein
HA	Human influenza hemagglutinin
HBSS	Hank's balanced salt solution
HSP	Hereditary Spastic Paraplegia
HIF-1α	Hypoxia-inducible factor-1
In	Input
IM	Inner membrane
IMS	Inner membrane space
IP	Immunoprecipitate
KO	Knock-out
LAMP2A	Lysosome-associated membrane protein 2A
LC3	microtubule-associated protein 1 light chain 3
m-AAA	Matrix-facing ATPase associated

MEF	Mouse Embryonic Fibroblast
MEF2	Myocyte enhancing factor 2
MOI	Multiplicity of Infection
MTS	Mitochondrial Targeting Sequence
OM	Outer membrane
PARL	Presenilin-associated rhomboid-like
PBS	Phosphate buffered saline
PINK1	PTEN-induced putative kinase 1
PEI	Poly(ethylenimine)
PVDF	Polyvinylidene fluoride
SCA	Spinal Cerebellar Ataxia
SDS	Sodium dodecyl sulphate
SDS-PAGE	Sodium dodecyl sulphate polyacrylamide gel electrophoresis
T-TBS	Tween 20 Tris-buffered saline
TM	Transmembrane
UPDRS	Unified Parkinsons Disease Rating scale
VHL	Von Hippel Lindau
WT	Wildtype

ACKNOWLEDGMENTS

I would first like to thank my supervisor Dr. David S. Park for his continued support and guidance throughout the term of my master's project. I am truly grateful for the opportunity he has given me to work within his lab and present my work at multiple conferences, including the 3rd Annual World Parkinson's Congress. I would also like to thank Dr. Alvin P. Joselin and Dr. M. Emdadul Haque for all their assistance, mentorship, training and advice over the duration of my term as a master's student. I must also thank Dr. Paul Marcogliese, M.Sc. Katherine Don-Carolis, Dr. Yasmilde Rodriguez Gonzalez, Dr. Elizabeth Abdel-Messih and our laboratory manager Steve Callaghan for their support and insightful discussions that were crucial in the development and troubleshooting of experiments for the duration of my projects. In addition, I would also like to give special thanks to the members of my advisory committee, Dr. Ruth Slack and Dr. Diane Lagace. Their support, knowledge, and discussions during our TAC meetings allowed me to have a better understanding of both my projects and importantly, helped shaped the direction of where they needed to go. I would also like to thank my family for their support and encouragement throughout my Master's degree. Especially my uncle Ricky Seegobin, who was pivotal in influencing my choice to pursue research in neuroscience and who passed away in February 2013 after surviving a spinal cord injury leaving him a quadriplegic for many years. Lastly, I would like to thank all the members of the Park lab. The collaborative environment could not have been more welcoming when I first entered the lab, and because of them I have reached where I am today.

INTRODUCTION

1. PARKINSON'S DISEASE

1.1 Relevance of Studying Parkinson's Disease

Parkinson's Disease (PD) is the most common neurodegenerative movement disorder that is characterized by many symptoms including akinesia, resting tremor, loss of balance and muscle stiffness (Kitada, Tong, Gautier, & Shen, 2009). In industrialized countries PD effects 0.3% of the population; having a mean age of onset at 60 with 1% of the total population affected over the age of 60; and 4% over the age of 80 (Dexter & Jenner, 2013). In Canada, over 55 000 Canadians have a diagnosis of PD, affecting almost 5% of all residents in long-term care facilities (Wong, Gilmore, & Ramage-Morin, 2014). PD is primarily prevalent within the older population, with 79% of PD patients in Canada 65 years of age or older (Wong et al., 2014). More so, as an age-related disorder, current population data predicts an increasing rate of PD prevalence due to an increasing older population. With current estimates that the Canadian population 65 years of age and older rising from 11.6% in 2012 to 23.6% in 2042; these facts highlight why understanding PD etiology is important to help develop treatments options for the increasing elderly that will develop PD (Canada, 2012).

1.2 Pathological Features of Parkinson's Disease

Since Dr. Parkinson's initial characterizations of the disease, significant improvement in the understanding of PD has been achieved (Parkinson, 2002). Through the post-mortem examination of the brains of PD patients, numerous pathological characteristics associated PD have been defined. More specifically, PD is often associated with 2 key pathological hallmarks. The primary and most well understood has

been the characterization of neuronal loss and decreased levels of dopamine production within the Substantia Nigra *pars compacta* (SNpc) located in the midbrain (Cookson, 2010; Dexter & Jenner, 2013). Resulting in decreased dopamine-mediated striatal activity, this is believed to be responsible for the classical motor symptoms experienced by PD patients.

In addition to the neuronal loss in the SNpc, the second most observed hallmark used in PD diagnosis is the presence of Lewy bodies and Lewy neurites (Moore, West, Dawson, & Dawson, 2005a). These bodies and neurites are comprised of abnormal protein rich spherical aggregates that can displace other cells within the brain, as well as localize along neuronal processes. These aggregates are normally found to contain a dense core surrounded by a halo of radiating filaments and have been identified within the SNpc region, and other regions associated with motor and non-motor symptoms such as the locus coeruleus and olfactory bulb (Dexter & Jenner, 2013; Witt et al., 2009). Although the presence of Lewy Bodies in the SNpc is characteristic of PD, their role in the pathogenesis of the disease remains poorly understood. Transgenic animal model studies have found the dominant protein contained within Lewy bodies and Lewy neurites, α-synuclein, is linked directly to the disease. As a result of this discovery, the scientific field has begun to adjust its view of PD as not simply a neurodegenerative disorder but also a synucleopathy (Dexter & Jenner, 2013).

1.3 Clinical Characterization of Parkinson's

Clinically, loss or reduced motor function is used as the main criteria to diagnose PD. The classical motor symptoms are loss of balance, changes in gait, difficulty with speech, resting tremor, stiffness, and bradykinesia (Dexter & Jenner, 2013; Jankovic, 2008). Resting tremor, often stereotypically linked to PD, can often decrease with directed movement and therefore symptoms can be temporarily eased when performing daily activities. Other symptoms such as bradykinesia (the slowness of movement), rigidity (an inherent increase in resistance to movement), and akinesia (absence of unconscious movement such as arm swings), often must be pharmacologically treated (Dauer & Przedborski, 2003). More so, these symptoms can often initially manifest asymmetrically but over time develop to become bilateral. The presentation of many of these symptoms is consistent with the clinical diagnosis of PD due to their association with basal ganglia dysfunction (Jankovic, 2008).

In order to better assess patients, scales have been developed that comparatively evaluate patients based on disease progression. One such scale is the Unified Parkinson's Disease Rating scale (UPDRS) (Jankovic, 2008). It allows for the examination of multiple motor symptoms, assessing 31 separate items. More so, when its reliability is compared with other scales developed to measure the disease and compared between patients, it has been considered one of the most valid and reliable scales ever used (Ramaker, Marinus, Stiggelbout, & Van Hilten, 2002).

In addition to the classical motor symptoms developed by PD patients, non-motor symptoms are becoming increasingly recognized as they impair quality of life. These can include increased apathy, depression, anosmia which is the loss in the ability to smell,

impaired executive function and reduced motivation (Haehner, Hummel, & Reichmann, 2011; Lelos et al., 2016). Disruptive sleep has also been associated with PD and is also predictive of developing PD. More specifically in 1996, REM Sleep Behavior Disorder was associated with an increased likelihood of PD diagnosis, with 38% of male patients diagnosed with REM Sleep Behavior Disorder being diagnosed with PD later in life (Schenck, Bundlie, & Mahowald, 1996).

1.4 Treatment of Parkinson's Disease

Although our understanding of the disease has greatly expanded, the complexity of PD and its symptoms often makes it difficult to treat. More so, due to the chronic neurodegenerative nature of the disease, PD becomes increasingly difficult to treat as time passes. However, treatment options do exist to help lessen patients' symptoms with the primary mechanism of treatment being dopamine replacement therapy. Treatment often begins with MAO-B inhibitors such as rasagiline which act to inhibit the degradation of dopamine, and have shown high tolerability among patients. If this treatment is not sufficient patients may progress to dopamine agonists such as rotigotine, ropinirole or pramipexole, or the drug Leva-Dopa, which is a precursor molecule to dopamine that can increase dopamine production and activity (Reichmann, 2016; Yahr, Duvoisin, Schear, Barrett, & Hoehn, 1969). For all of these treatments, known side-effects exists which often reduce compliance among patients. For example, dopamine agonists have been linked to impulse control disorders, such as binge eating, pathological gambling or excessive shopping (Reichmann, 2016). Additionally, L-Dopa treatment is only effective for a short period and after 2-5 years of sustained use many patients report

a decrease in the duration of effectiveness to relieving their symptoms, commonly termed "wearing off" (Antonini et al., 2011).

1.5 Genetics of Parkinson's Disease

Environmental and genetic factors are believed to play a major role in PD. PD has been associated to mutations within specific genes, resulting in familial of PD. Amongst familial PD, mutations or duplications of the SNCA gene, producing α-synuclein, or mutations within LRRK2 are associated with autosomal dominant familial PD (Burbulla & Krüger, 2011; Moore et al., 2005b). In contrast, mutations in the genes which have been the focus of our work, PARK7, PARK6 and PARK2, which code for the proteins DJ-1, PTEN Induced Kinase 1 (PINK1), and Parkin are associated with autosomal recessive PD (Kitada et al., 2009; Moore et al., 2005b). Parkin was initially identified by an exon 4 deletion leading to juvenile PD in a Japanese family (Kitada et al., 1998). DJ-1 was first identified in an Italian family, with the L166P missense mutation being associated with early onset PD (Bonifati et al., 2003). For PINK1, a variety of mutations linked to disease onset have been identified. One such mutation is the D525fsX562 frameshift mutation which is linked to early onset PD, and has been associated with symptoms as early as age 9 (Roh et al., 2004). Identification of these genetic links have allowed both *in vitro* and *in vivo* models to be developed. However, though heritable mutations have been linked to disease onset, in particular autosomal recessive forms to early onset PD, the mechanistic roles in disease pathogenesis of these proteins have yet to be elucidated.

2. AUTOPHAGY

2.1 Mechanisms of Autophagy

Autophagy, derived from the Latin reference for self-eating, defines the biological process for catabolism of proteins and organelles within the cell. Of this process, there are 3 main variations, microautophagy, macroautophagy and chaperone mediated autophagy (Harris & Rubinsztein, 2011). Microautophagy refers to the direct uptake of cytosolic components into a lysosome and is often considered a targeted degradation mechanism although it has not been examined extensively (Reggiori & Klionsky, 2002; Rubinsztein, 2006). Macroautophagy is the process of membrane formation and engulfment of cytosolic components, and often termed the process of bulk protein degradation (Ahmed et al., 2012; Reggiori & Klionsky, 2002). In comparison, chaperone mediated autophagy is a highly selective process of protein degradation. Through chaperone mediated autophagy, cytosolic proteins containing the KFERQ peptide motif are selectively degraded by binding the chaperone HSC70. Through interaction with lysosome-associated membrane protein 2A (LAMP2A), chaperone bound proteins are then transferred to LAMP2A and imported directly into the lysosomal lumen where they can be digested and their constituents reused (Rubinsztein, 2006).

2.2 Molecular mechanisms in PD pathogenesis

In studying the function of heritable PD mutations, we have begun to understand PD has a complex pathogenesis. Two common associations identified through these examination have been the role of oxidative stress and dysregulated autophagy in PD etiology. DJ-1 in particular has been linked to the cellular response to oxidative stress.

For example, DJ-1 null cortical neurons and mice are hypersensitive to oxidative insult by both H_2O_2 and MPTP treatment respectively. Additionally, this phenotype can be rescued by DJ-1 expression, suggesting DJ-1's neuroprotective function in response to oxidative stress (R. Kim et al., 2005). DJ's function in detecting oxidative stress is thought to be mediated by DJ-1 oxidation at Cysteine 106 (Canet-Avilés et al., 2004). An additional mechanism by which DJ-1 exerts its protective effect is through its ability to modulate the neuronally protective pathway mediated by AKT phosphorylation. DJ-1 is involved in the recruitment of AKT to the membrane following oxidative stress (Aleyasin et al., 2010). More recently we have also found DJ-1 to interact with the protein Von Hippel Lindau (VHL), a E3 ubiquitin ligase similar to Parkin (Parsanejad, Zhang, et al., 2014b). Here, DJ-1 negatively regulates VHL's interaction with its substrate hypoxia inducible factor 1 (HIF-1α), a neuroprotective transcription factor primarily involved with response to oxidative stress. This lead DJ-1 deficiency to result in decreased HIF-1α under oxidative stress, and the presence of DJ-1 to increase HIF-1α by reducing degradation occurring by VHL ubiquitination, allowing for HIF-1α mediated neuroprotection (Parsanejad, Zhang, et al., 2014b). PINK1 has also been demonstrated to have a protective function in response to oxidative stress with studies showing H_2O_2 treatment triggering TRAP1 phosphorylation by PINK1, leading to decreased pro-apoptotic cytochrome C release. Importantly this activity was not observed in PD linked mutant variants G309D and L347P (Pridgeon, Olzmann, Chin, & Li, 2007). This would suggest PINK1 phosphorylation activity may increase survival under increased cellular stress conditions.

The biological process of autophagy was initially associated with PD pathogenesis after PD histological analysis illustrated the formation of α-synuclein protein-rich aggregates known as Lewy bodies (Ahmed et al., 2012). More recent examinations have linked PD to autophagic activity at a molecular level. One pathway has been through PD-linked genes PINK and Parkin, and their role in regulation of autophagy of damaged mitochondria, termed mitophagy. Illustrated through many studies, PINK1 kinase activity can recruit the E3-ubiquitin ligase Parkin to damaged mitochondria, and initiating and regulating the process of mitochondrial clearance (Karbowski & Youle, 2011; Youle & Narendra, 2010). Where in *in-vivo* models of *Drosophila M*. examined, Parkin deficiency resulted in significantly decreased mitochondrial clearance. Similarly, PD-linked mutations within kinase domain of PINK1 inhibited Parkin translocation to damaged mitochondria, and restricted autophagic activity (Song et al., 2013; Vincow et al., 2013).

In addition to mitophagy, chaperone mediated autophagy (CMA) is associated to PD as specific proteins are targeted selectively for degradation. One of those proteins is myocyte enhancing factor 2 (MEF2), a transcription factor which functions in neuronal survival and who's mutations and loss of function have been associated with Alzheimer's disease (Gong et al., 2003; González et al., 2007). Through CMA, WT and PD-linked mutants of α-synuclein can significantly disrupt the interaction of MEF2D with the chaperone HSC70, a key component in CMA, resulting in increased levels of non-functional MEF2D (Yang et al., 2009). Therefore with increased levels of WT and PD-linked mutant forms of α-synuclein in PD patient samples also demonstrating increased levels of MEF2D, not only does this further suggest CMA's regulatory role, it provides a

specific mechanism for autophagy's role in PD pathogenesis (Irrcher & Park, 2009; Yang et al., 2009).

2.3 Macroautophagy

Macroautophagy, herein referred to as autophagy, is the process of bulk protein degradation within the cell facilitating the turnover of misfolded and damaged proteins and organelles (Ahmed et al., 2012). In this process, damaged proteins and organelles are sequestered by multiple molecular markers into autophagosomes.

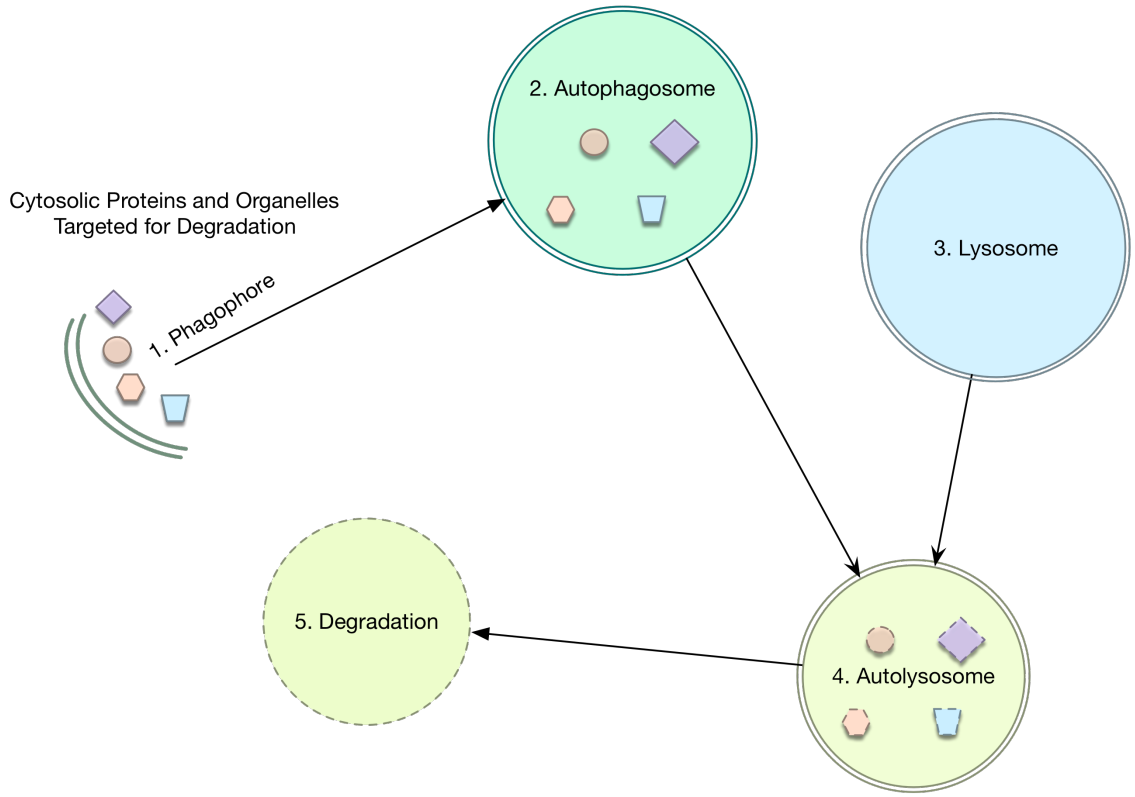

Figure 1. Illustration of 5 major stages within the macroautophagy pathway. Based on (Ashrafi & Schwarz, 2012; Mizushima & Komatsu, 2011).

As illustrated in Figure 1, damaged proteins and organelles are sequestered during a *de novo* double-membrane vesicle known as the phagophore or omegasome (Mizushima,

Yoshimori, & Ohsumi, 2011; Xie & Klionsky, 2007). In this process the damaged proteins and organelles become encapsulated into the forming autophagosome. Through the merger of the autophagosome with the lysosome (also termed autolysosome), contents within begin to breakdown allowing for them to be recycled and exported to be used for other cellular processes (Mizushima & Komatsu, 2011).

2.4 ATG5-ATG12-ATG16 Complex Formation

During autophagosome formation, many proteins are involved in developing the phagophore and allowing for encapsulation of organelles and proteins targeted for degradation. These include ATG5, ATG12, ATG7, ATG10, LC3-I, LC3-II, and ATG16 (where ATG refers to autophagy related). Each of these proteins plays a vital function during the early autophagy process (Figure 2).

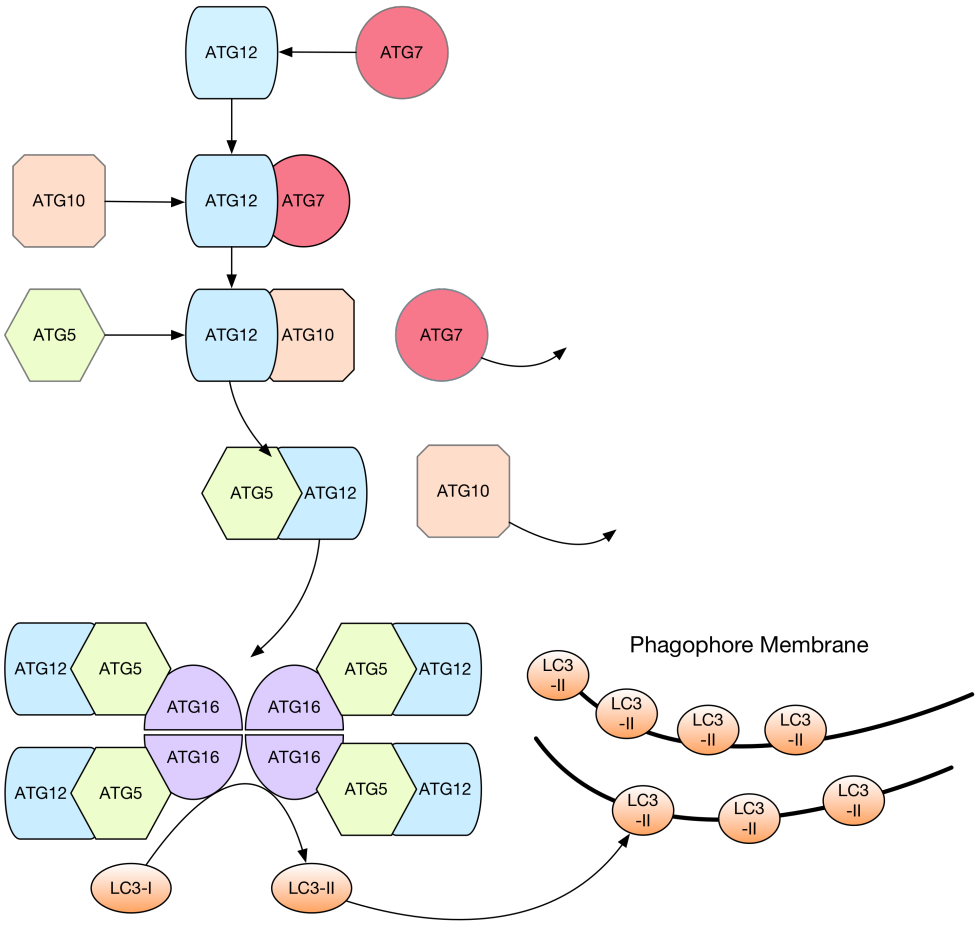

Figure 2. Illustration of the formation of the ATG5-ATG12-ATG16 protein complex required for the formation LC3-II involved in early autophagy during phagophore formation. Based on (Mizushima, Yoshimori, & Ohsumi, 2003; Wang & Klionsky, 2003)**.**

As illustrated in Figure 2, in the early stages, ATG12 is activated by ATG7, an E1 like enzyme, through esterification. This allows for the transfer of ATG12 to the E2 ligase enzyme ATG10 via an isopeptide bond. Following this conjugation, ATG10 transfers ATG12 to ATG5 forming a stable isopeptide bond that allows for the formation of the major conjugate ATG5-ATG12. This conjugate can then interact with ATG16 forming the functional multimeric protein complex, facilitating the formation of LC3-II

from LC3-I. Similarly, yeast homologues ATG5 and ATG12 form a conjugate and function as an E3-like ligase catalyzing the lipidation of ATG8, homologous to LC3, to ATG8-phosphatidylethanolamine (ATG8-PE) on the phagophore membrane. Therefore in a similar process, LC3-I is believed to be conjugated to a currently unknown lipophilic substrate allowing it to form LC3-II (Hanada et al., 2007; Mizushima et al., 2003; Sou et al., 2008; Wang & Klionsky, 2003).

2.5 DJ-1 and Autophagy

In 2010, our lab showed that DJ-1 deficiency leads to an increase in autophagic flux in mouse embryonic fibroblasts (MEFs). This was demonstrated by a decrease in LC3-II and protein p62/sequestosome 1 (p62) as well as restoration of LC3-II levels after bafilomycin A1 treatment (Irrcher et al., 2010). Selected cytoplasmic components can localize to the forming autophagosome via p62-LC3 binding with degradation after autophagosome maturation and lysosomal membrane fusion (Klionsky, 2007; Klionsky et al., 2008; Lim et al., 2011). Therefore LC3 and p62 serve as critical markers of autophagic activity (Kabeya et al., 2000; Klionsky, 2007; Mizushima, Levine, Cuervo, & Klionsky, 2008; Sou et al., 2008). Consistent with these observations in MEFs, decreased levels of autophagic marker p62 was also observed in lymphoblast samples collected from patients diagnosed with DJ-1 linked PD indicating that an increase in autophagic flux may be a marker of disease pathogenesis (Irrcher et al., 2010).

Autophagy has been shown to play a significant role in cell survival, especially in models of neurodegenerative disease; however to date, we have had no mechanistic understanding of how DJ-1 deficiency might lead to altered autophagic flux.

Accordingly, to further explore this important phenomenon, we undertook an unbiased approach in collaboration with Figeys *et al.* using a co-immunoprecipitation-mass spectrometry analysis to identify novel interactors of DJ-1. Through this approach we identified two autophagy related gene candidates: ATG5 (APG5) and ATG12 (APG12), both key regulators of early autophagy, as potential interactors of DJ-1.

We hypothesized that DJ-1 under normal conditions interacts with the autophagy system through ATG5 and ATG12, and participates in its regulation through inhibition of conjugate activity. Therefore, in patients suffering with PD, such as in DJ-1 linked familiar forms, loss of DJ-1 activity may lead to increased autophagy, thus sensitizing neurons to stress and cell death.

3. PINK1 AND AFG3L2

3.1 PINK1 Structure

PINK1 is a 62 Kilodalton (Kd) protein consisting of 581 amino acid (aa) with 4 defined domains and 1 region containing the mitochondrial targeting sequence (MTS) and predicted cleavage sites spanning the first 103 aa (Figure 3). These domains include the MTS, transmembrane domain, serine/threonine kinase domain and the C-terminal domain. Within these regions, multiple mutations have been linked to the onset of Parkinson's disease such as G309D, W437X, D525fsX562 and C92F. Importantly, some mutations such as C92F are localized within regions where PINK1 is known to be processed and cleaved away, such as by PARL at position 103 (Deas et al., 2011; Greene et al., 2012). Therefore, these findings question the importance of PINK1 fragments in context to PINK1 basal function that is also not well understood.

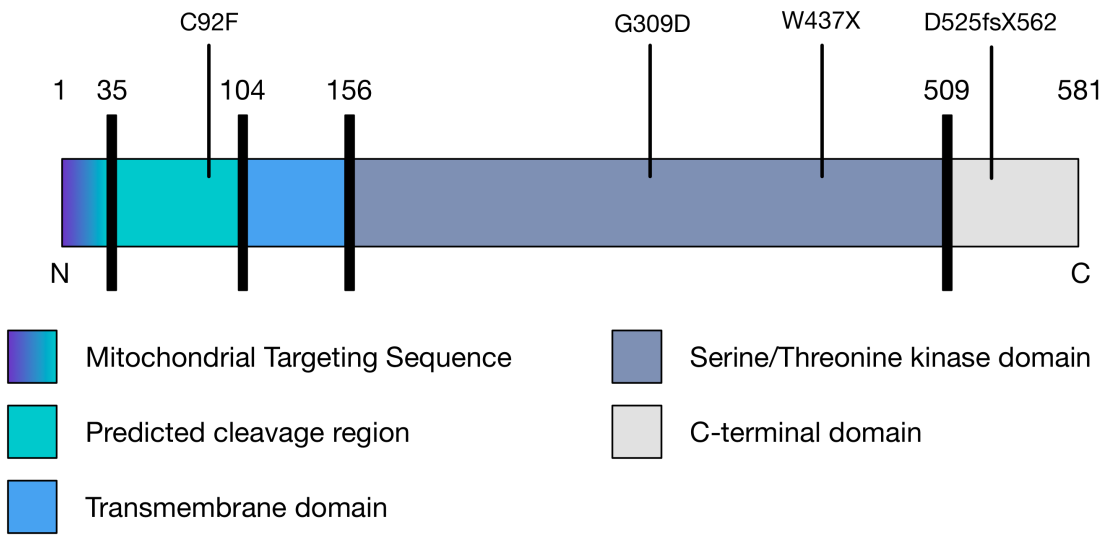

Figure 3. PTEN Induced Kinase 1 (PINK1) protein structure. Regions defined from N to C terminus are mitochondrial targeting sequence (1-35aa), predicted cleavage region (1-103aa), transmembrane domain (104-155aa) serine/threonine kinase domain (156-508aa), and C-terminal domain (509-581aa). C92F, G309D, W437X and D525fsX562 positions indicate select known PD associated mutations of PINK1. Based from (Becker, Richter, Tocilescu, Przedborski, & Voos, 2012; Deas et al., 2011; Greene et al., 2012).

3.2 PINK1 Function under Mitochondrial Stress

Previous examinations of PINK1 and Parkin have begun to elucidate their cellular function. This is especially true under stressful cellular conditions with their role in the identification and degradation of damaged mitochondria through the selective autophagic process known as mitophagy. When mitochondria are damaged, PINK1 has been found to accumulate on the outer-mitochondrial membrane (OMM) interacting with the TOM7 complex (Hasson et al., 2013). PINK1 can then signal Parkin, an E3 ubiquitin-like ligase, to translocate to the mitochondria via its own kinase function through ubiquitin phosphorylation at Serine-65 (Kane et al., 2014). This has been shown in HEK293 cell cultures treated with mitochondrial uncoupler carbonyl cyanide m-

chlorophenylhydrazone (CCCP) to result in the translocation of cytosolic Parkin to the mitochondrial membrane as well as confirmed in mouse cortical neurons (Joselin et al., 2012; Narendra, Tanaka, Suen, & Youle, 2008). Subsequent studies show that the translocation of Parkin mediates the degradation of the mitochondria via Parkin's ubiquitin ligase activity, allowing for the ubiquitination of OMM proteins, targetting the mitochondria to autophagic machinery and beginning the mitophagic process (Cai, Zakaria, Simone, & Sheng, 2012; Kane et al., 2014; Narendra et al., 2008).

3.3 PINK1 Basal Function

In comparison to examination under stressful conditions, basal PINK1 function is less well understood. Under basal conditions, PINK1 is targeted to the mitochondrial membrane. Dependent on the mitochondrial membrane potential, an indication of mitochondrial health, PINK1 is imported into the inner mitochondrial matrix by both TOM and TIM23 protein complexes (Becker et al., 2012; Jin et al., 2010). Once imported, PINK1 is cleaved by mitochondrial processing peptidase (MPP), followed by presenilin-associated rhomboid-like protease (PARL) and potentially other unknown proteins including our hypothesized protease, AFG3L2. This leads to multiple cleavage products that can localize both within the mitochondria and cytosol following export where it can be finally degraded (Deas et al., 2011; Greene et al., 2012; Lin & Kang, 2008). Many studies have suggested cleaved PINK1 may play a role within the cytoplasm prior to degradation, since PINK1 cleavage products are exported (Lin & Kang, 2008; Takatori, Ito, & Iwatsubo, 2008). However in studies examining PINK1, following cleavage PINK1 degradation is accelerated. Mediated by the ubiquitin-proteasome

pathway, that can be inhibited by MG132, cleavage of PINK1 leads to rapid turnover as evident by pulse-chase examination over a short 2-hour period (Lin & Kang, 2008). This would indicate that PINK1 processing is a degradation mechanism. However, other studies demonstrate PINK1 performing basal functions, in particular regulating mitochondrial activity. This would suggest prior to export, mitochondrial cleavage may be more than simply a stage of PINK1 degradation. In earlier examinations identifying PINK1 localization, PINK1 has been found to integrate into the inner mitochondrial membrane following import (Lin & Kang, 2008; Pridgeon et al., 2007). In examining PINK1 knockout cells, we have also shown PINK1 to play a role regulating Complex I function by mediating the phosphorylation of its subunit NdufA10 (Morais et al., 2014). Loss of this phosphorylation results in mitochondrial depolarization and decreased ATP synthesis (Morais et al., 2014; 2009). Consistent with earlier studies, PINK1 null astrocytes also showed decreased proliferation and AKT activation, with proliferation deficits mediated by a total decrease in mitochondrial mass, mitochondrial function and integrity (Choi et al., 2013). And through prior examination by our lab, it was demonstrated that a N-terminal deletion mutant of PINK1 demonstrates neuroprotective effects from oxidative stress (Haque et al., 2008). Taking these studies as a whole, as well as our examinations of PINK1 null mice resulting in increased sensitization of dopaminergic neurons to MPTP treatment *in vivo*, a second mass spectrometry screen in collaboration with Figeys *et al.* was conducted identifying potential protein interactors of PINK1 (Haque et al., 2012). As a result of the screen, one highly intriguing interacting protein candidate was identified: AFG3L2.

3.4 AFG3L2

AFG3L2 is a mitochondrial m-AAA protease located on the inner mitochondrial membrane (IMM) that can form both homo- and hetero-oligomeric complexes. In humans, complexes are formed with family members paraplegin and additionally in mice with AFG3L1, with the hexameric complex's functional protease domain facing the matrix-side of the mitochondria (Almajan et al., 2012; Kremmidiotis et al., 2001).

As a 797aa metalloprotease, AFG3L2 contains 2 major domains, with the primary domain being its M41 family peptidase, and the second being its ATPase Associated with diverse cellular Activities (AAA) domain binding ATP to power its peptidase function (Löbbe et al., 2013). Additionally, AFG3L2 has also been shown to exert chaperone-like activity facilitating proper formation of mitochondrial Complex 1 involved in respiration (Luigia Atorino, 2003). On its own, mutations within AFG3L2 protease domain are linked to a neurological disorder known as Spinal Cerebellar Ataxia (SCA) Type 28 (Almajan et al., 2012). However, in reference to AFG3L2's known function to hetero-oligomerize with family member paraplegin, it has also been associated with the disorder Hereditary Spastic Paraplegia (HSP). Interestingly, both disorders result in symptoms similar to PD with gait abnormalities. However HSP patients also manifest symptoms of lower-limb ataxia and dysarthria, with pathogenesis mediated by retrograde degeneration of motor axons (Mancuso, Barth, Pietro P Crivello, & Rugarli, 2012).

MATERIALS AND METHODS

4.1 Antibodies

Western blot and immunoprecipitation were performed using primary antibody including anti-DJ-1 (Abcam), anti-ATG5 C-terminus (Abgent), anti-ATG12 [2011S] (Cell-signaling), anti-myc-tag (Abcam), anti-Flag (Sigma), anti-GRP75/mHSP70 [JG1] (Abcam), anti-p62 (American Research Products) and anti-LC3 (Novus Biologicals).

4.2 Cell culture

HEK293, HeLa, and MEF cells lines were propagated in sterile cell culture under 37°C at 5.0% CO_2 conditions. Cells were maintained in Dulbecco's modified Eagle's medium (DMEM), high glucose containing 10% FBS and 1% antibiotic/antimicotic (ABAM).

4.3 Transgenic Mice Lines

DJ-1 WT and KO Mice were generated and maintained as described previously on a C57Bl/6 (Charles River) background (R. Kim et al., 2005; Rousseaux et al., n.d.). We obtained transgenic heterozygous AFG3L2$^{+/Emv66}$ mice on the Balbc strain, characterized previously (Maltecca et al., 2008) were provided by Dr. Gregory Cox. Heterozygous AFG3L2$^{+/Emv66}$ mice were crossed with over-expressing C57Bl/6N Crj GFP-LC3 mice which were provided by Dr. Diane Lagace (Mizushima, Yamamoto, Matsui, Yoshimori, & Ohsumi, 2004). Offspring mice were maintained as an inbred mixed line, and crossed to generate an AFG3L2$^{+/Emv66}$ / GFP-LC3 homozygous line. Mice were then crossed to be used for embryonic cortical dissection. All mice were housed at the University of Ottawa Animal Care and Veterinary Services vivarium. Animal care was carried out in

accordance with the guidelines of the Canadian Council and Care of Animals in Research and was approved by the University of Ottawa Animal Care Veterinary Services.

4.4 Mice and Genotyping

Embryonic tail samples from AFG3L2 mice were collected at time of dissection in preparation of cortical neuronal cultures. AFG3L2, DJ-1 transgenic and AFG3L2--LC3-GFP double transgenic mice ear samples were collected at weaning. Samples were digested in genomic DNA lysis buffer (0.1M Tris [pH 8.5], 5mM EDTA, 0.2% SDS, 0.2M NaCl) by Proteinase K at 0.2 mg/mL for 30 minutes at 55°C. DNA was then diluted 10x in H_2O, boiled for 3 minutes and separated from debris by centrifugation at 14,000 RPM for 3 minutes. PCR was performed to detect the WT or KO allele for DJ-1 (DJ-1 forward primer: TGC TGA AAC TCT GCC ATG TGA ACC, DJ-1 reverse primer: CCT GCT TGC CGA ATA TCA T, and Neo Cassette: AGG TGA CAC TGC CAG TTG CTA GTC); WT or KO allele for AFG3L2 (U3-LTR forward primer: CCA GAA ACT GTC TCA AGG TTC C, R25 reverse primer: TGG ATT CTG CAC ATC TCT TAA CCC, and R25 forward primer: GGA ACT GAC CAT ATC TGG TTG TCT G) and presence or absence of LC3-GFP allele (GFP forward: TCC TGC TGG AGT TCG TGA CCG, LC3 reverse: TTG CGA ATT CTC AGC CGT CTT CAT CTC TCT CGC, mLC3ex3GT forward: TGA GCG AGC TCA TCA AGA TAA TCA GGT, mLC3ex4AG reverse: GTT AGC ATT GAG CTG CAA GCG CCG TCT)

4.5 Cortical neuronal dissection and culture

Cortical neurons were prepared as previously described (Joselin et al., 2012). Briefly, dissection of mouse embryos occurred at 15-16 days gestation. Cortical tissue was then digested using 0.5mg/ml trypsin in Hank's balanced salt solution (HBSS) for 25 minutes at 37°C while shaking. Digestion was stopped by the addition of Neurobasal media containing 0.2mg/ml trypsin inhibitor and 0.2mg/ml DNaseI. Neurons were then triturated, and isolated by centrifugation twice at 1200rpm for 5 minutes at 4°C. Neurons were then resuspended in complete Neurobasal media containing B-27, N-2, Pen-Strep and L-Glutamine and plated into Poly-D-Lysine coated plates.

4.6 Co-Immunoprecipitation

HEK293 cells were transiently transfected using PEI (Polysciences Inc.) with recombinant constructs expressing either myc-ATG5 (Addgene), myc-ATG12 (Addgene), or Flag-DJ-1.

WT DJ-1 MEF cell were transiently infected with adenoviral constructs containing Flag-DJ-1, Flag-DJ-1 (L166P), Flag-DJ-1 (C106A) and EGFP control. MOI adjusted per virus to equilibrate for infection efficiency determined by EGFP expression under control of a second promoter in DJ-1 viral vectors. 24 hours post transfection protein lysates were independently harvested by cell-scraping and mechanical lysis in IP lysis buffer (50mM Tris HCl [pH 7.4], 1mM EDTA, 100mM NaCl and 0-1% Nonidet P-40 as indicated) supplemented with EDTA-Free Halt Protease Inhibitor Cocktail (Thermo Scientific).

Adult whole WT and KO DJ-1 mouse brain samples were homogenized in lysis buffer (50 mM Tris-HCl [pH 7.4], 100 mM NaCl, 1 mM EDTA, 1 mM DTT, and 0.2% Triton X-100) with EDTA-Free Halt Protease Inhibitor Cocktail and pre-cleared with anti-rabbit TrueBlot© Ig IP beads at 4°C for 1 hour. Cellular debris was cleared by centrifugation at 10, 000 RPM at 4°C for 10 minutes. Cleared lysate was collected and primary antibody incubation was performed through incubation with either anti-myc-tag (Abcam), anti-DJ-1 (Abcam), or anti-FLAG-tag (Sigma-Aldrich) antibody overnight at 4°C. Immunoprecipitation of endogenous, myc-tagged and FLAG-tagged proteins were performed using TrueBlot© Ig IP beads (eBiosciences) respectively at 4°C for 1 hr. Following incubation, beads were washed three times in lysis buffer without protease inhibitors with final elution of immunoprecipitated proteins conducted through the addition of 30uL 2x SDS sample buffer (2.2% SDS, 8% Glycerol, 0.08M Tris HCl [pH 6.8], 0.02% Bromophenolblue, 2% β-mercapto-ethanol).

4.7 SDS-PAGE and Western Blot

Proteins samples were quantified by Bradford assay using manufacturer's (BioRad) protocol. Post quantification, samples were mixed with 5x SDS sample buffer (5.5% SDS, 16% Glycerol, 0.3M Tris HCl [pH 6.8], 0.1% Bromophenolblue, 2% β-mercapto-ethanol) and then separated by PAGE using gels containing either 12% or a 10-18% acrylamide gradient and then transferred to a PVDF membrane. The membrane blots were then blocked in 5% milk for 30 minutes at room temperature and incubated with targeted primary antibody. Antibody incubation was performed with 2.5% BSA either for 1 hour at room temperature or 4°C overnight. Membranes were washed 3 times with

TBS-T solution for 10 minutes and incubated with secondary IgG antibody in 5% milk for 1 hour at room temperature. Following incubation, membranes were washed 3 times with TBS-T and protein levels were assessed by Pierce™ ECL Western Blotting Substrate.

4.8 Live-cell imaging

Cortical neurons derived from E15-16 GFP-LC3 positive, WT or KO AFG3L2 mice were incubated on ice post-dissection for 40 minutes and plated onto PDL-coated glass bottom plates at a concentration of 150,000 neurons in 400uL per plate. At 2 Days *in-vitro* (DIV) neurons were infected with lentiviral vector expressing mitochondrial label OCT-DsRed and maintained in 2mL of complete neurobasal media. At 6 DIV Neurobasal media was changed to complete neurobasal media without B27. 7 DIV immediately prior to imaging live neurons were treated with 1:2000 dilution of Hoechst (Thermo-Fisher Scientific) for nuclear staining immediately prior to imaging on the Quorum WaveFX-X1 spinning disk confocal microscope using the 63x oil-immersion Leica objective for a period of 2 hours at 37°C with 5% CO_2 with images taken at 3 minutes intervals.

4.9 Mitochondria-enriched membrane fraction isolation and lysis

10 cm cell culture plates containing confluent AFG3L2 WT and KO MEFs were harvested and the membrane fraction was isolated through subcellular fractionation in an isolation buffer (0.25M Sucrose, 10mM Tris [pH 7.5], 1mM EDTA) by successive centrifugation as described previously (Greene et al., 2012). The supernatant (cytosol) was removed from the pelleted mitochondria enriched membrane fraction. The

mitochondria were lysed by pulse sonication for 30 seconds on ice in m-AAA protease buffer (20mM HEPES [pH 7.4], 50mM NaCl, 1mM ZnCl, 2% Triton X-100, 5mM $MgCl_2$), reaction buffer conditions previously established by (Nolden et al., 2005). Mitochondrial lysates were then concentrated by centrifugation at (11,000 x g, 10 minutes) in Amicon® Ultra 0.5mL 30kd centrifugal filters (Millipore).

4.10 PINK1-Flag purification

HeLa cells were infected with PINK1-Flag adenovirus in DMEM with 2% FBS and 1% antibiotic/antimicotic. 18 hours post infection, cells were treated with 1µM CCCP for 24 hrs and then harvested. The cells were washed twice in PBS and pelleted by centrifugation. Cellular lysis in lysis buffer (20 mM Tris-HCl [pH 7.9], 500 mM NaCl, 4mM $MgCl_2$, 0.4 mM EDTA, 20mM β-glycerophosphate, 20% glycerol, 1 mM DTT with complete protease inhibitors) was achieved by 3 subsequent freeze/thaw cycles in liquid nitrogen. Cellular debris was then pelleted by centrifugation at 8000 RPM for 15 minutes at 4°C. Supernatant containing PINK1-Flag was then incubated with 250µl bed volume anti-Flag M2 affinity gel (Sigma) equilibrated in lysis buffer on a rotator for 4 hours at 4°C. PINK1 bound Flag-M2 beads were washed 4 times in lysis buffer containing 0.5mM DTT and complete protease inhibitor. Bound PINK1-Flag proteins were eluted using a Flag-peptide solution (200µg/ml 3x Flag-peptide, 0.5mM DTT with complete protease inhibitor) by 3 successive incubations of 250µl Flag-peptide solution on a rotator for 20 minutes at 4°C. Eluted PINK1-Flag proteins were pooled, mixed with lysis buffer and concentrated at 14,000 x g for 10 minutes at 4°C in Amicon® Ultra

0.5mL 30kd centrifugal filters (Millipore). Concentrated immunopurified PINK1-Flag protein was then aliquoted and stored at -80°C.

4.11 *In vitro* PINK1-Flag cleavage assay

Concentrated immunopurified PINK1-Flag was mixed with m-AAA protease buffer (20mM HEPES [pH 7.4], 50mM NaCl, 1mM ZnCl, 2% Triton X-100, 5mM $MgCl_2$) and buffered exchanged in Amicon Ultra 0.5mL 30kd centrifugal filters at 11,000 x g for 10 minutes (Millipore). PINK1-Flag protein was then collected and equally mixed with previously prepared lysed mitochondria derived from AFG3L2 WT and KO MEFs in m-AAA protease buffer, with PINK1-Flag alone in m-AAA protease buffer as control. The reaction was initiated by the addition of 1 mM fresh and samples were incubated at 30°C for 60 minutes. The reactions were stopped by the addition of 5x SDS sample buffer and boiling for 3 minutes, and then samples were stored at -80°C.

4.12 *In vitro* PINK1-Flag stabilization assay

Using similar conditions to the PINK1-flag cleavage assay, described in 4.10, concentrated immunopurified PINK1-Flag was mixed with m-AAA protease buffer (20mM HEPES [pH 7.4], 50mM NaCl, 1mM ZnCl, 2% Triton X-100, 5mM $MgCl_2$) and buffered exchanged in Amicon Ultra 0.5mL 30kd centrifugal filters at 11,000 x g for 10 minutes (Millipore). PINK1-Flag protein was then collected and equally mixed with 20ng, 60ng, or 80ng of human recombinant AFG3L2-GST protein (Abnova) or 80ng GST protein eluted from GST-beads as control. The reaction was initiated by the addition of 1 mM fresh and samples were incubated at 30°C for 60 minutes. The reactions were

stopped by the addition of 5x SDS sample buffer and boiling for 3 minutes, and then samples were stored at -80°C.

4.13 MTS-PINK1-HA fragment plasmid construct generation

Recombinant PINK1-hemagglutinin (HA) tagged WT and fragment-containing constructs were generated using WT full-length human PINK1. WT and fragments were cloned into a pAdtrack vector with their expression and GFP expression under control of a second CMV promoter as a positive reporter. Three recombinant constructs were generated, full-length PINK1-HA, MTS-Δ104-PINK1-HA, and hypothetical PINK1-fragment MTS-Δ154-PINK1-HA. Full-length human recombinant PINK1 was generated to contain the HA-tag along the C-terminal end. MTS-Δ104-PINK1-HA construct, representing PARL cleavage at position 104, was customized to contain the first 35aa of WT-PINK1 representing the N-terminal MTS. Following the 35aa, a Δ104-PINK1-HA fragment exists. MTS-Δ154-PINK1-HA construct representing a hypothetical PINK1 N-terminal cleavage product was generated to contain the first 35aa of WT-PINK1 representing the N-terminal MTS. Following the MTS, a Δ154 PINK1 fragment followed by HA-tag exists. To generate the HA-tag, mutation of the WT stop codon to a glycine was performed. Once constructed, plasmids were transformed into Invitrogen OneShot™ Stbl3 chemically competent *E*. coli bacterial cells and amplified for plasmid purification.

4.14 Statistical analysis

Statistical analysis was conducted as indicated by either a one-tailed or two-tailed unpaired student t-test or two-way analysis of variance (ANOVA) between means with significance achieved if p-value was less than 0.05.

RESULTS

Assessing the interaction of DJ-1 with autophagy related proteins ATG5 and ATG12

5.1 DJ-1 does not co-immunoprecipitate with ATG5 or ATG12

As a result of the mass spectrometry screen conducted in collaboration with Dr. Daniel Figeys, ATG5 and ATG12 were identified as interacting partners of DJ-1 (Ewing et al., 2007). To confirm this interaction, a co-immunoprecipitation experiment was performed. Myc-ATG5 or myc-ATG12 was overexpressed in HEK293 cells and immunoprecipitated using a myc antibody to detect their interaction with endogenous DJ-1. However, no noticeable interaction with endogenous DJ-1 was observed (Figure 4).

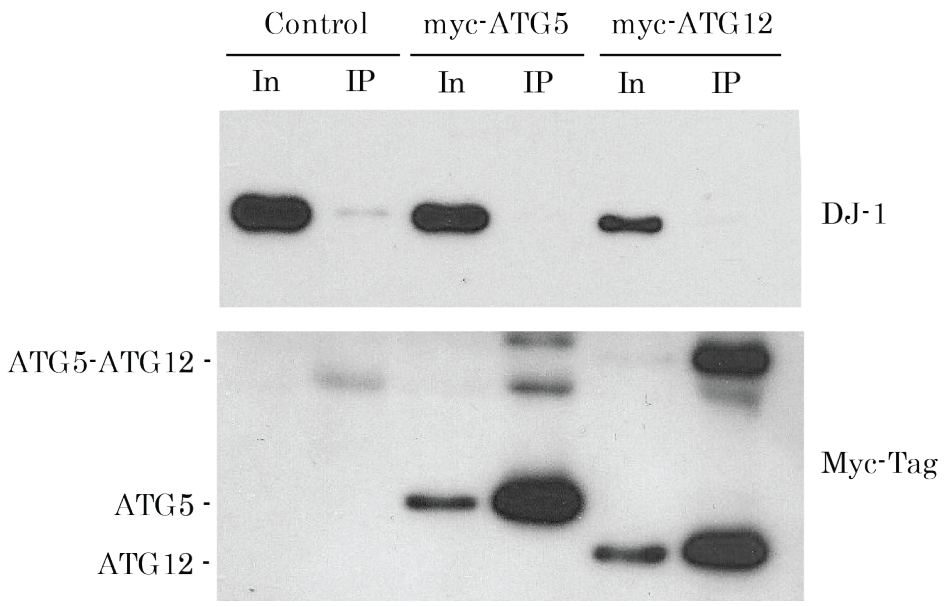

Figure 4. Immunoprecipitation of DJ-1 in HEK293 cell cultures transfected with myc-tagged ATG5, ATG12, or empty-vector control. Cells harvested in IP lysis buffer (0.5% Nonidet P-40). Immunoprecipitations were performed through incubation of anti-myc-tag antibody overnight followed by incubation with anti-rabbit IgG conjugated Protein A/G beads (eBiosciences). Empty vector pCMV-3-Tag-2 was used as a control. Top panel: Immunoblot of DJ-1 by anti-DJ-1 (Abcam); Bottom panel: Immunoblot of overexpressed protein using myc-tag antibody.

In order to test whether induction of autophagy may play a role in the interaction, HEK293 cells were modestly starved by 4hr EBSS treatment after transfection with myc-ATG5, myc-ATG12 or both constructs. However, even under conditions of starvation, enhancing autophagy, no interaction between overexpressed myc-ATG5, myc-ATG12 and endogenous DJ-1 was detected (Figure 5).

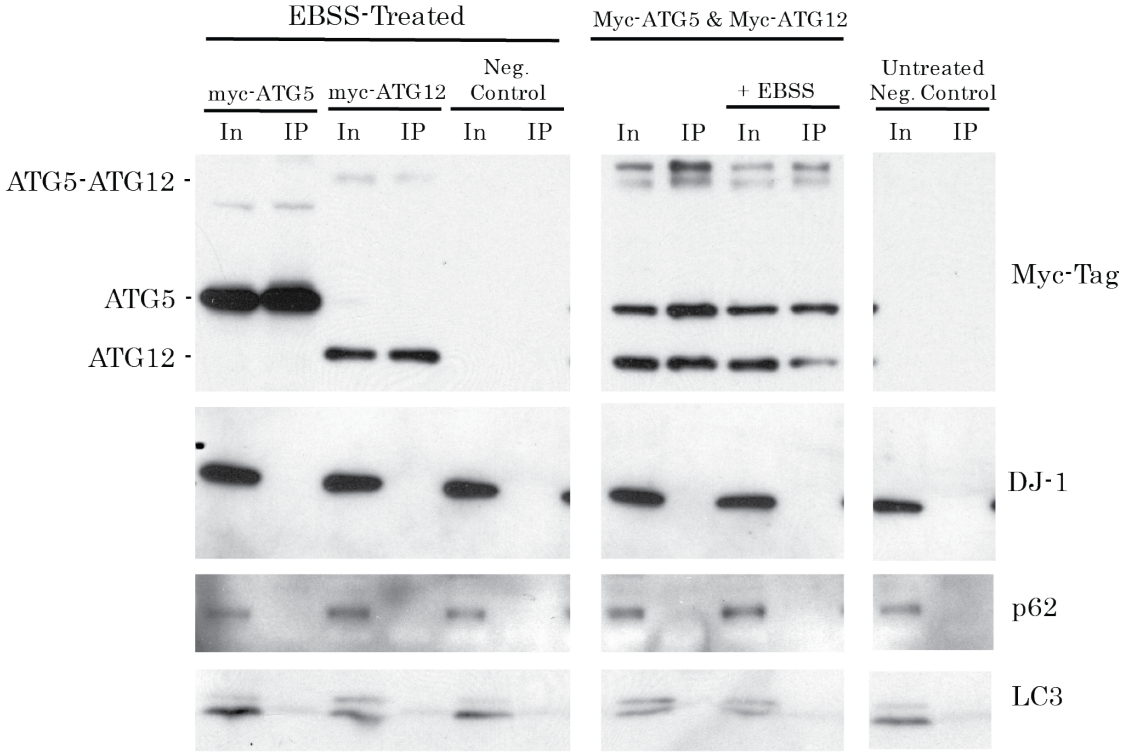

Figure 5. Immunoprecipitation of DJ-1 in HEK293 cell cultures transfected with myc-tagged ATG5, ATG12, or empty-vector control treated with EBSS for 4 hours. Cells harvested in IP lysis buffer (0.5% Nonidet P-40). Immunoprecipitations were performed through incubation of anti-myc-tag antibody overnight followed by incubation with anti-rabbit Ig IP beads (eBiosciences). EBSS treated negative control represented by expression of empty pCMV-3-Tag-2 myc-tag vector. Untreated negative control represented by co-expression of empty pCMV-3-Tag-2 myc-tag vector and pEGFP-C2 vector. Immunoblot of DJ-1 by anti-DJ-1 (Abcam).

To resolve whether the interaction may be limited to total DJ-1 protein levels, constructs containing myc-ATG5, myc-ATG12 and Flag-DJ-1 were co-expressed in

HEK293 cells. However, over-expression of myc-ATG5, myc-ATG12 & Flag-DJ-1 we were unable to co-immunoprecipitate Flag-DJ-1, with DJ-1 detected by anti-Flag-tag (Figure 6).

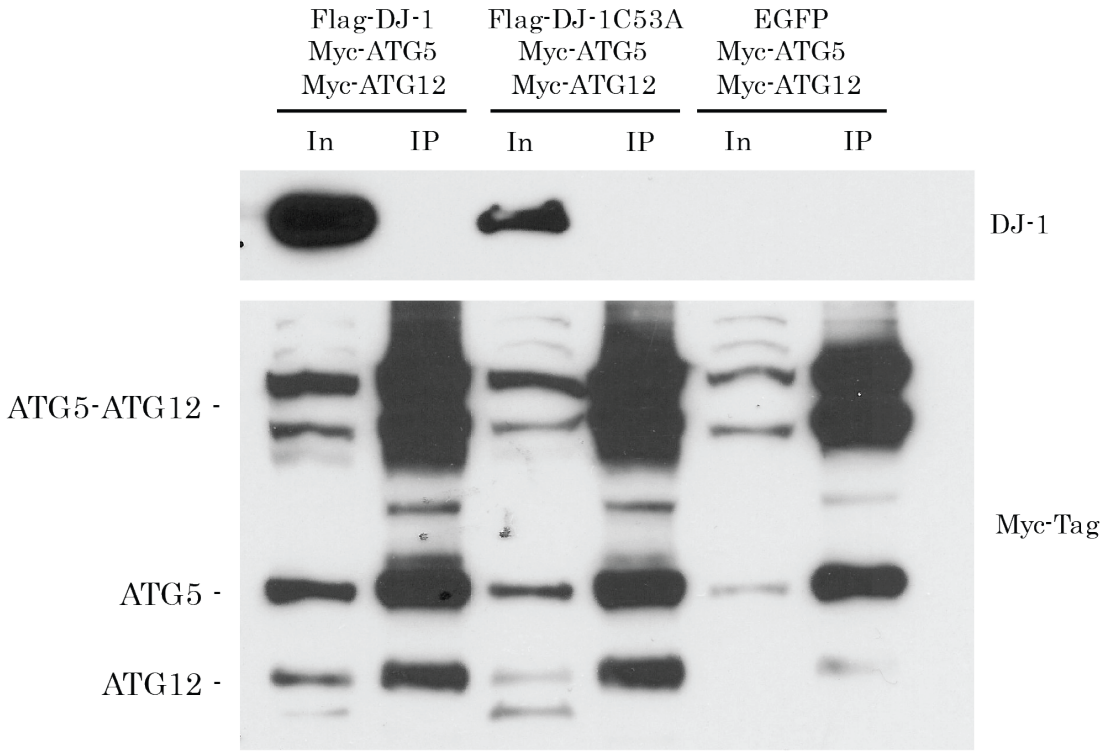

Figure 6. Immunoprecipitation of DJ-1 in HEK293 cell cultures co-transfected with myc-tagged ATG5, ATG12 and Flag-DJ-1, or Flag-DJ-1 (C53A) mutant. Cells were harvested in lysis buffer (0.5% Nonidet P-40). Immunoprecipitations were performed through incubation of anti-myc-tag antibody overnight followed by incubation with anti-rabbit Ig IP beads (eBiosciences). Top panel: Immunoblot detection of DJ-1 by anti-Flag (Sigma). Bottom panel: Immunoblot detection of overexpressed proteins by anti-myc-tag.

To address whether co-immunoprecipitation by anti-myc-tag may be inadequate in elucidating the interaction, a reverse IP was performed using an anti-Flag-tag antibody. WT MEFs were infected with recombinant Adeno-virus expressing Flag-DJ-1, Parkinson-linked mutant DJ-1 L166P, or DJ-1 C106A, and anti-oxidant deficient DJ-1 mutant followed by Flag-tag immunoprecipitation. Infection efficiency was monitored by

the expression of EGFP under the control of a separate promoter. In DJ-1 L166P infected cells, infection was confirmed by GFP expression, though DJ-1 L166P was not detected by anti-DJ-1, likely due to its known decreased stability. Although DJ-1 immunoprecipitation was successful in Flag-DJ-1 and DJ-1 C106A infected cells, we could not immunoprecipitate endogenous ATG5 or ATG5-ATG12 in WT MEFs (Figure 7).

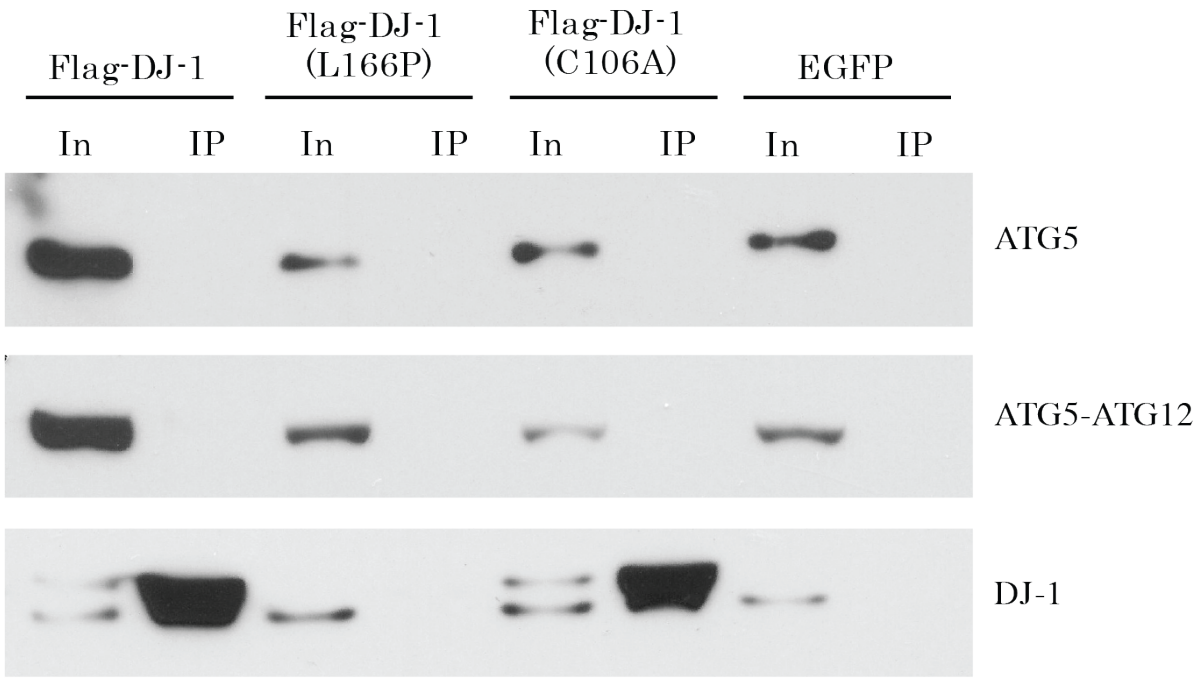

Figure 7. Immunoprecipitation of ATG5 and ATG12 in DJ-1 wildtype MEFs cultures adeno-virally infected with Flag-DJ-1, Flag-DJ-1 (L166P) mutant, Flag-DJ-1 (C106A) mutant or EGFP virus control. Cells were harvested in lysis buffer (0-0.5% Nonidet P-40). Immunoprecipitations were performed through incubation of anti-Flag (Sigma) antibody overnight followed by incubation with anti-mouse Ig IP beads (eBiosciences). Immunoblot detection of DJ-1 by anti-DJ-1 (Abcam).

To determine whether ATG5, ATG12 and DJ-1 proteins levels play a significant role in the detection of interaction, we over-expressed myc-ATG5, myc-ATG12 and Flag-DJ-1 in HEK293 cells followed by anti-Flag-tag immunoprecipitation. However,

with expression of myc-ATG5, myc-ATG12 & Flag-DJ-1, we were unable to conclusively co-immunoprecipitate myc-ATG5 or myc-ATG12 after anti-Flag incubation, with non-specific pull down shown with our controls (Figure 8).

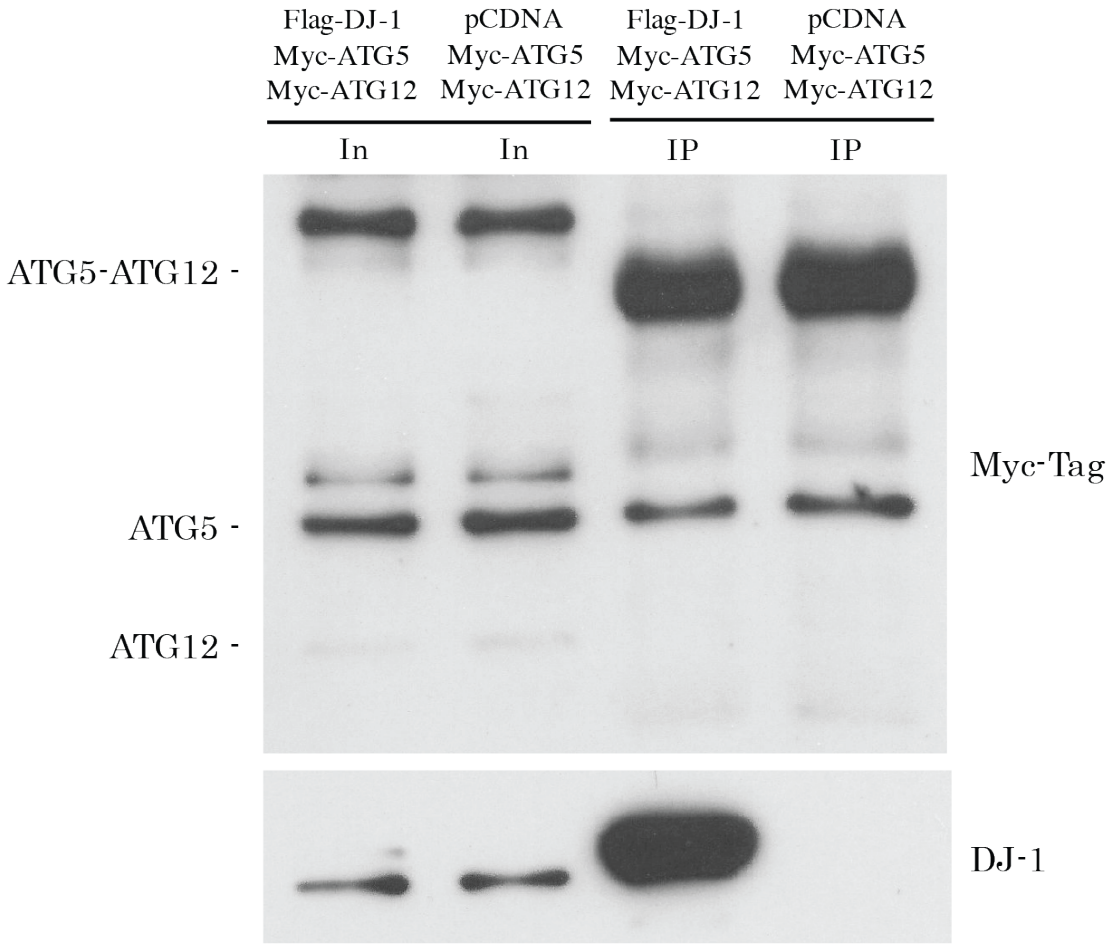

Figure 8. Immunoprecipitation of myc-ATG5 and myc-ATG12 in HEK293 cell cultures co-transfected with myc-tagged ATG5, ATG12 and Flag-DJ-1 or empty pCDNA vector control. Cells were harvested in lysis buffer (50mM Tris HCl [pH 7.4], 1mM EDTA, 100mM NaCl and 0% Nonidet P-40). Samples pre-cleared with TrueBlot© Ig IP beads prior to immunoprecipitation by incubation of anti-flag (Sigma) antibody overnight. Immunoblot detection of DJ-1 by anti-DJ-1 (Abcam).

Although our initial goal was to confirm the mass-spectrometry screen conducted in HEK293 cells by over-expressing our protein of interest, since this did not work we attempted, to use whole brain lysates. Whole brain lysates can provide many advantages,

such as a larger amount of protein but maintain DJ-1, ATG5 and ATG12 at endogenous protein levels. Additionally, whole brain lysates would likely provide a more relevant model of interaction in PD than HEK293 cells. Therefore, DJ-1 WT and KO adult mice were dissected and whole brain lysates were incubated with anti-DJ-1 to elucidate whether DJ-1 may co-immunoprecipitate with ATG5, ATG12 or both. Our results from DJ-1 immunoprecipitation with whole murine brains could not conclusively co-immunoprecipitate endogenous ATG5 or ATG5-ATG12, with non-specific pulldown in DJ-1 KO brain samples.

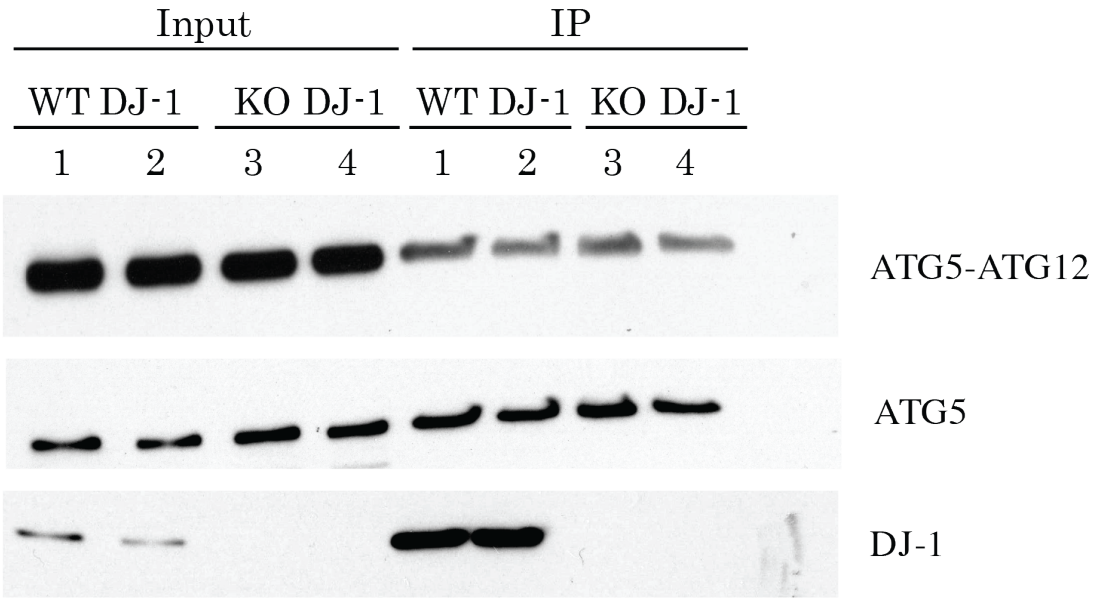

Figure 9. Endogenous co-immunoprecipitation of ATG5 and ATG12 from DJ-1 wildtype or knockout whole murine brain samples after DJ-1 pull-down. Adult DJ-1 wild-type and DJ-1 knockout control animals were dissected with whole brains extracted and mechanically homogenized in IP lysis buffer (50mM Tris HCl [pH 7.4], 1mM EDTA, 0.5mM DTT, 100mM NaCl, 0.2% Nonidet P-40). Protein lysates were pre-cleared with TrueBlot© anti-mouse Ig IP beads (eBiosciences). DJ-1 immunoprecipitation and detection were performed through incubation of anti-DJ-1 (Abcam) antibody.

AFG3L2 mediates PINK1 processing, and stability, as PINK1 fragments rescues AFG3L2 deficiency

5.1 AFG3L2 Deficiency upon PINK1

Through initial examination of PINK1 and its potential interaction with AFG3L2, we were able to successfully elucidate the interaction between AFG3L2 and PINK1. This was performed through the expression and co-immunoprecipitation of recombinant human myc-AFG3L2 and PINK1-Flag protein constructs as shown in Figure 10 (Joselin *et al.*, unpublished).

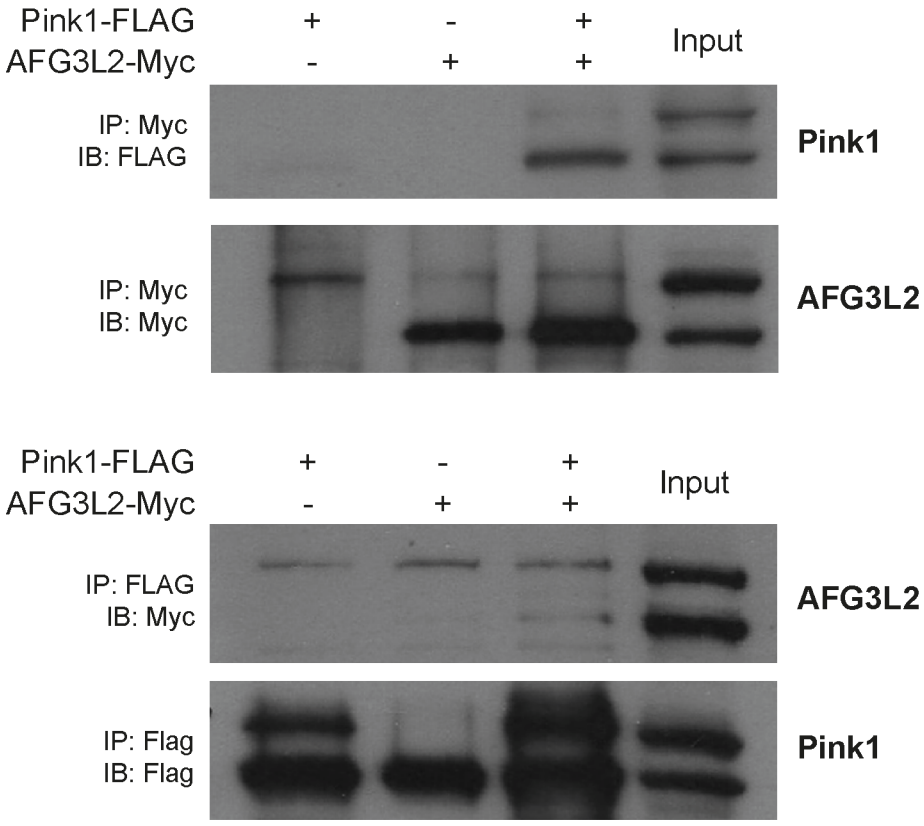

Figure 10. Forward and reverse co-immunoprecipitation of recombinant AFG3L2-myc interacting with PINK1-flag. Recombinant proteins were over-expressed in HEK293A cell culture and immunoprecipitated with either anti-Flag-tag or anti-myc antibodies. Adapted from Joselin *et al.*, unpublished.

Following this, Dr. Joselin *et al.* examined how AFG3L2 itself may effect PINK1, particularly since AFG3L2 is known to have both active protease and chaperone-like activity. Using AFG3L2 deficient mouse embryonic fibroblasts (MEFs), differential cleavage of exogenously expressed PINK1-Flag was observed along with decreased total PINK1 protein levels as a result of AFG3L2 deficiency. This was also confirmed in murine cortical neurons as seen in Figure 11.

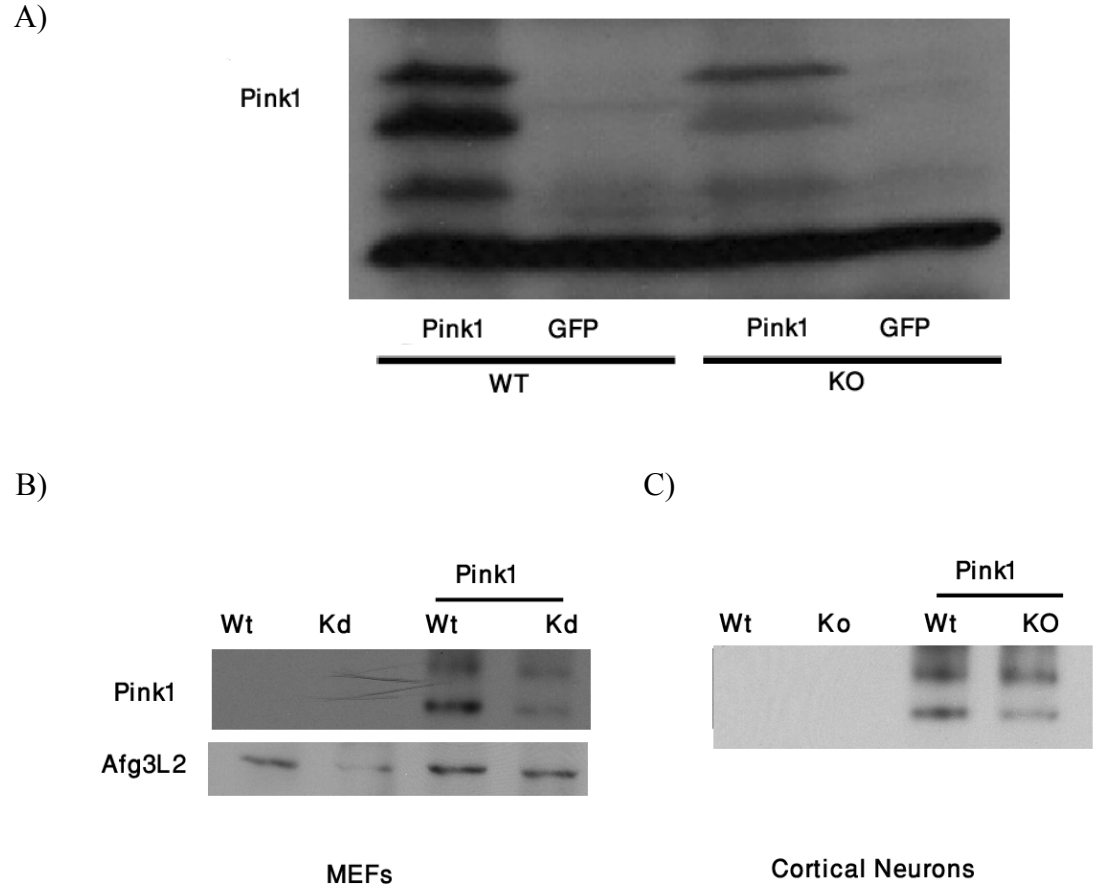

Figure 11. Differentially processed and decreased stability of PINK1-flag mediated by AFG3L2 deficiency in MEFs and murine cortical neurons. A) AFG3L2 knock-out (KO) mouse embryonic fibroblasts (MEFs) compared to AFG3L2 wildtype with GFP vector expression as control and B) AFG3L2 acute knock-down (Kd) in MEFs and C) AFG3L2 wildtype cortical neuronal cultures with PINK1 detected by anti-Flag. Adapted from Joselin *et al.*, unpublished.

Based on these observations, I hypothesized that AFG3L2 partially mediates PINK1 processing and this processing is required to maintain mitochondrial integrity. Therefore, in AFG3L2 deficient cells, improper processing of PINK1 was predicted to result in the loss of PINK1 basal function leading to loss of mitochondrial integrity, mitochondrial depolarization and stabilization of full-length PINK1 on the OMM. This would trigger the translocation of Parkin to the mitochondria and activation of the mitophagy pathway (Narendra et al., 2008).

5.2 PINK1 is differentially processed by AFG3L2 deficient mitochondria

In order to better comprehend the functional interaction of PINK1 with AFG3L2, and AFG3L2's role as a m-AAA protease, an *in vitro* cleavage assay was developed using buffer conditions established previously with MPP (Nolden et al., 2005). AFG3L2 is naturally found to be functional when in an oligomeric structure stabilized on the mitochondrial membrane, which is difficult to mimic using purified protein (Ramelot et al., 2013). Thus, to examine enzymatically active AFG3L2, our methodology employed lysis of a mitochondria-enriched fraction isolated by sub-cellular fractionation of AFG3L2 WT and KO MEF's. Our examination excitingly revealed purified PINK1-Flag was differentially cleaved *in vitro* by AFG3L2 WT mitochondria, generating an approximately 35kd product compared to AFG3L2 KO mitochondrial controls (Figure 12). Since this assay was performed using a mitochondrial lysate versus the purified protein complex, AFG3L2 may not exclusively mediate the cleavage observed due to the large number of mitochondrial proteases present. However, this result in combination

with our previous work (Figure 11) supports that AFG3L2 is directly involved in mediating PINK1 processing.

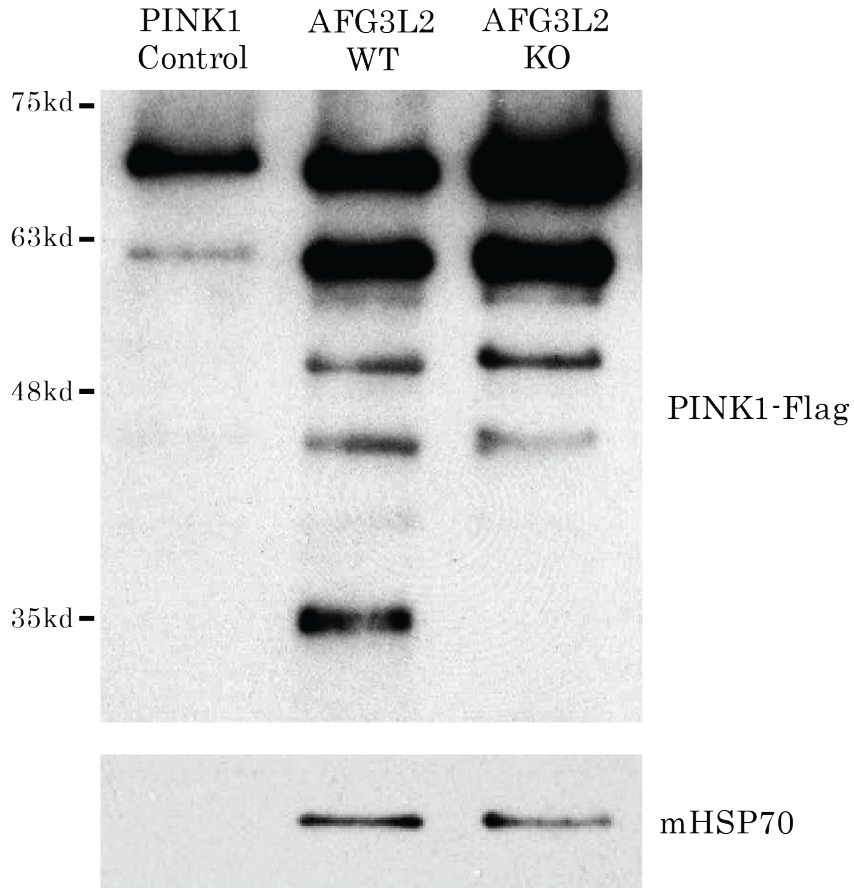

Figure 12. Differential cleavage *in vitro* of immuno-purified PINK1-Flag by isolated and lysed WT AFG3L2 mitochondria compared to KO AFG3L2 mitochondrial control. Top panel: Immunoblot detection by antibody incubation with anti-flag (Sigma) with PINK1 control containing no mitochondrial lysate. Bottom panel: Immunoblot detection of mitochondrial mHSP70 by anti-Grp75/mHSP70 [JG1] (Abcam).

5.3 AFG3L2 stabilizes PINK1

In our previous examinations of PINK1-Flag overexpression in AFG3L2 WT and KO MEFs, there was decreased cleavage of PINK1, and a decrease in total PINK1 protein levels in AFG3L2 KO cells (Figure 11). As AFG3L2 is also known to have

chaperone-like activity (Arlt, Tauer, Feldmann, Neupert, & Langer, 1996), we hypothesized that PINK1 proteins levels may be additionally stabilized by AFG3L2.

To test this function, commercially purified human recombinant AFG3L2-GST protein was obtained and incubated with purified human PINK1-Flag *in vitro* using buffer conditions similar to the *in vitro* cleavage assay described previously, with 80ng purified GST protein as control (Figure 13). Knowing functional cleavage can only occur by hexameric complex formation, monomeric purified AFG3L2 protein should exhibit no cleavage activity, and thus in this assay only AFG3L2 stabilization-like function would be examined (Almajan et al., 2012; Luigia Atorino, 2003). The results of this experiment revealed PINK1-Flag stabilization by human recombinant AFG3L2-GST protein, compared to the equivalent 80ng GST protein control. This suggests AFG3L2 may also function to stabilize PINK1 within the mitochondria, potentially regulating its endogenous function.

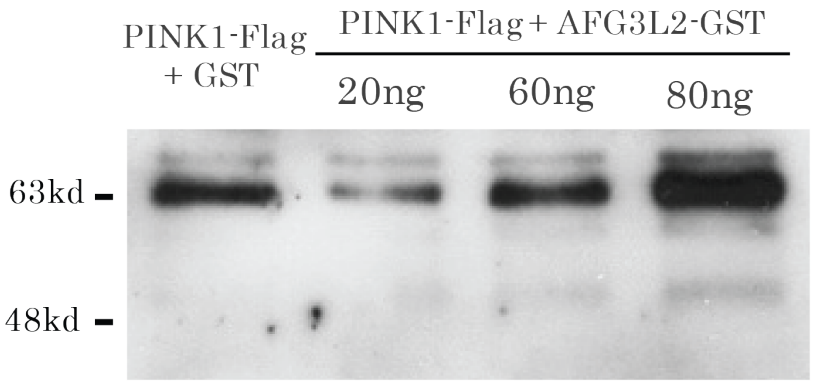

Figure 13. *In vitro* stabilization of purified human PINK1-Flag by human recombinant AFG3L2-GST compared to GST protein control. 20ng, 60ng and 80ng refer to total AFG3L2-GST protein incubated with PINK1 protein. 80ng GST protein used as control. Immunoblot detection of PINK1-Flag by antibody incubation with anti-flag (Sigma).

5.4 AFG3L2 deficiency demonstrates increased endogenous mitophagy

PINK1 has been linked by many research groups to be involved in signalling mitochondrial damage and triggering mitochondrial clearance via mitophagy (Jin & Youle, 2013; Okatsu et al., 2012). AFG3L2 loss has also previously been shown to result in mitochondrial damage and fragmentation (Ehses et al., 2009; Maltecca et al., 2012). Based on these findings and given the fact that we detected a functional impact of AFG3L2 on PINK1 cleavage and stability, it was important to understand how loss of AFG3L2 may impact PINK1's role in mitophagy.

To observe endogenous mitophagy in MEFs, AFG3L2 WT and KO MEFs were experimentally examined by Joselin *et al.* under naïve and after 4 hour bafilomycin treatment (Figure 14). Bafilomycin inhibits late-stage autophagy, and allows for the examination of autophagic flux by preserving autophagosomes through inhibiting degradation. By quantifying co-labelled mitochondria, with mitochondria labelled by anti-MTCO1 (Complex IV, subunit 1) being cleared to remain within autophagosome labelled by autophagy marker anti-LC3 we can examine the flux of mitophagy occurring. This experiment demonstrated significantly increased mitophagy in both naïve and after bafilomycin treatment. This would indicate damage by loss of AFG3L2 can significantly activate the mitophagic pathway, likely mediated by PINK1 activity.

A)

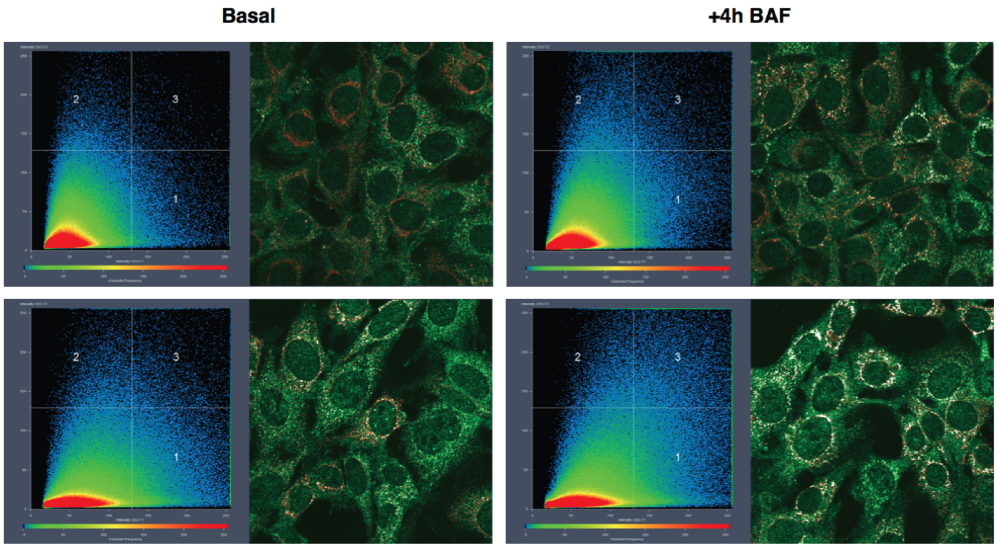

B)

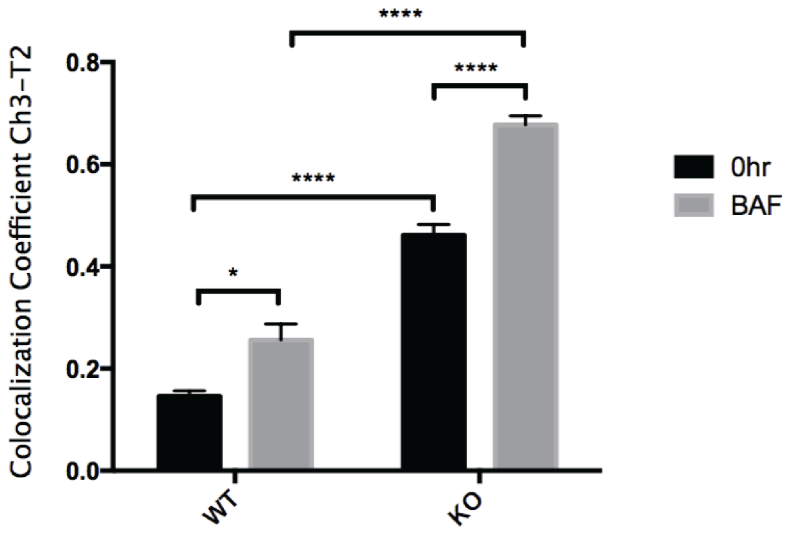

Source of Variation	P value	P value summary	Significant?
Interaction	0.0195	*	Yes
AFG3L2 deficiency	< 0.0001	****	Yes
Baf treatment	< 0.0001	****	Yes

Figure 14. Endogenous mitophagy in AFG3L2 WT and KO murine embryonic fibroblasts after 4hrs bafilomycin treatment. AFG3L3 WT and KO MEFs were treated with 300nm bafilomycin for 4 hrs and fixed by 4% PFA. Mitochondria labeled by anti-MTCO1 (Complex IV, subunit 1) and autophagosomes labelled by anti-LC3. A) Graph of Mander's co-localization of mitochondria by anti-MTCO1 (Red) and autophagosomes by anti-LC3 (Green) with area 3 representing co-localized pixels per group. B) Statistical analysis was conducted by assessing Mander's Coefficient of co-localisation of anti-MTCO1 with anti-LC3 by two-way ANOVA. Data collected and analysed by Joselin *et al.* N = 5.

As indicated previously, AFG3L2 loss has previously been shown to result in increased mitochondrial damage illustrated by fragmentation (Maltecca et al., 2012). Therefore, with an observable increase in MEF mitophagy, it was important to understand if mitochondrial morphology was also compromised in our AFG3L2 KO cortical neurons, previously found in purkinje neurons in previous studies (Almajan et al., 2012). Analysis of AFG3L2 cortical neurons for endogenous mitochondrial fragmentation (Figure 15A) revealed a significant increase in mitochondrial fragmentation in AFG3L2 KO murine cortical neurons (Figure 15B). With experiments conducted and analysed by Joselin *et al*., this would suggest our AFG3L2 KO neurons recapitulate the phenotype of mitochondrial damage as a result of AFG3L2 deficiency.

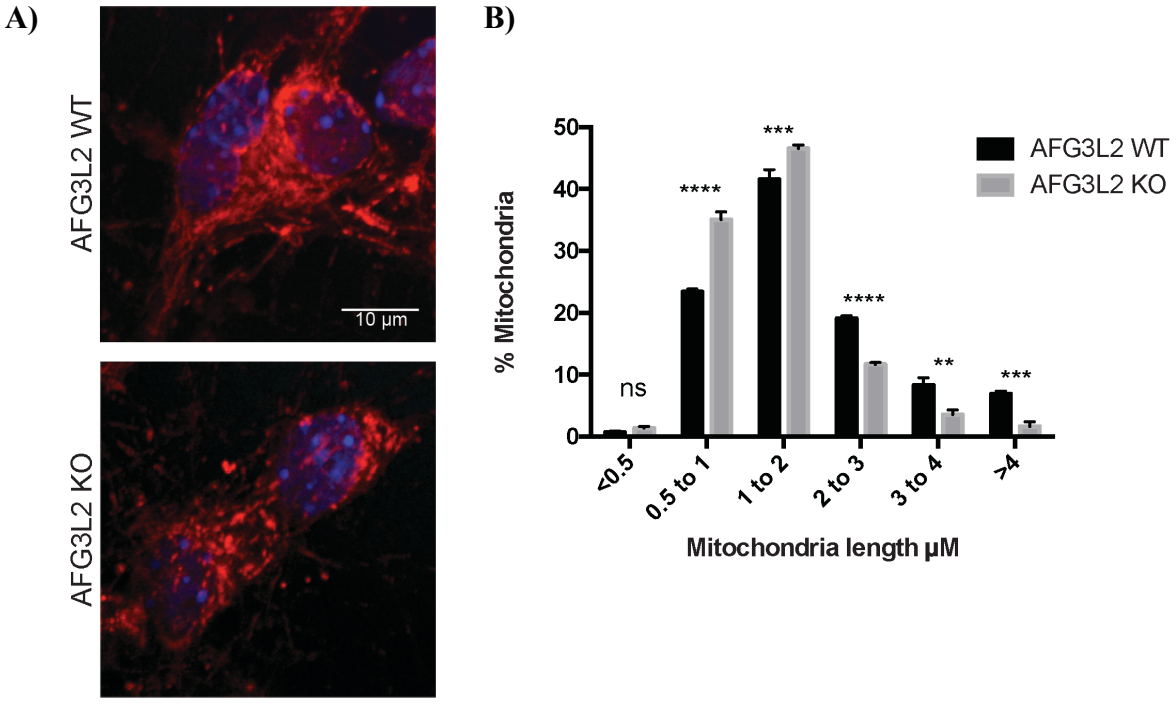

Figure 15. Mitochondrial length of AFG3L2 WT and KO murine cortical neurons. A) E15-16 neurons were cultured for 6-7 DIV and fixed by 3.7% formalin. Mitochondria (Red) were labelled by anti-MTCO1 with nucleus labeled by Hoechst (Blue). B) Distribution of mitochondrial length between AFG3L2 WT and KO neurons. Significance calculated by two-way ANOVA. N = 400. Data collected and analysed by Joselin *et al.*

With our results suggesting increased mitophagy in MEFs (Figure 14), and an indication that AFG3L2 loss results in increased neuronal mitochondrial fragmentation (Figure 15), it was important to assess mitophagy within a neuronal system that may be more relevant to PD. Therefore we generated a double-transgenic GFP-LC3/AFG3L2 mouse line that could allow us to better understand the impact of AFG3L2 loss within primary cultured murine cortical neurons. To examine active mitophagy, live-cell imaging was employed to assess co-localization of mitochondria (labelled by OCT-DsRed lenti-virus infection) with GFP-LC3 (autophagic marker) as a criteria for mitophagy. Assessment was done in GFP-LC3 positive and AFG3L2 WT (Figure 16A)

or KO (Figure 16B) cortical neurons. This examination revealed GFP-LC3/AFG3L2 KO neurons had active, endogenous mitophagy (Figure 16C) with co-localization events in a range of 1-4 events per neuron observed (Figure 16D). In WT neurons, no co-localization events observed (Figure 16A). Although we cannot conclude our results statistically as no events were observed in WT neurons, our data would suggest loss of AFG3L2 may result in increased active endogenous mitophagy in double-transgenic neurons.

A)

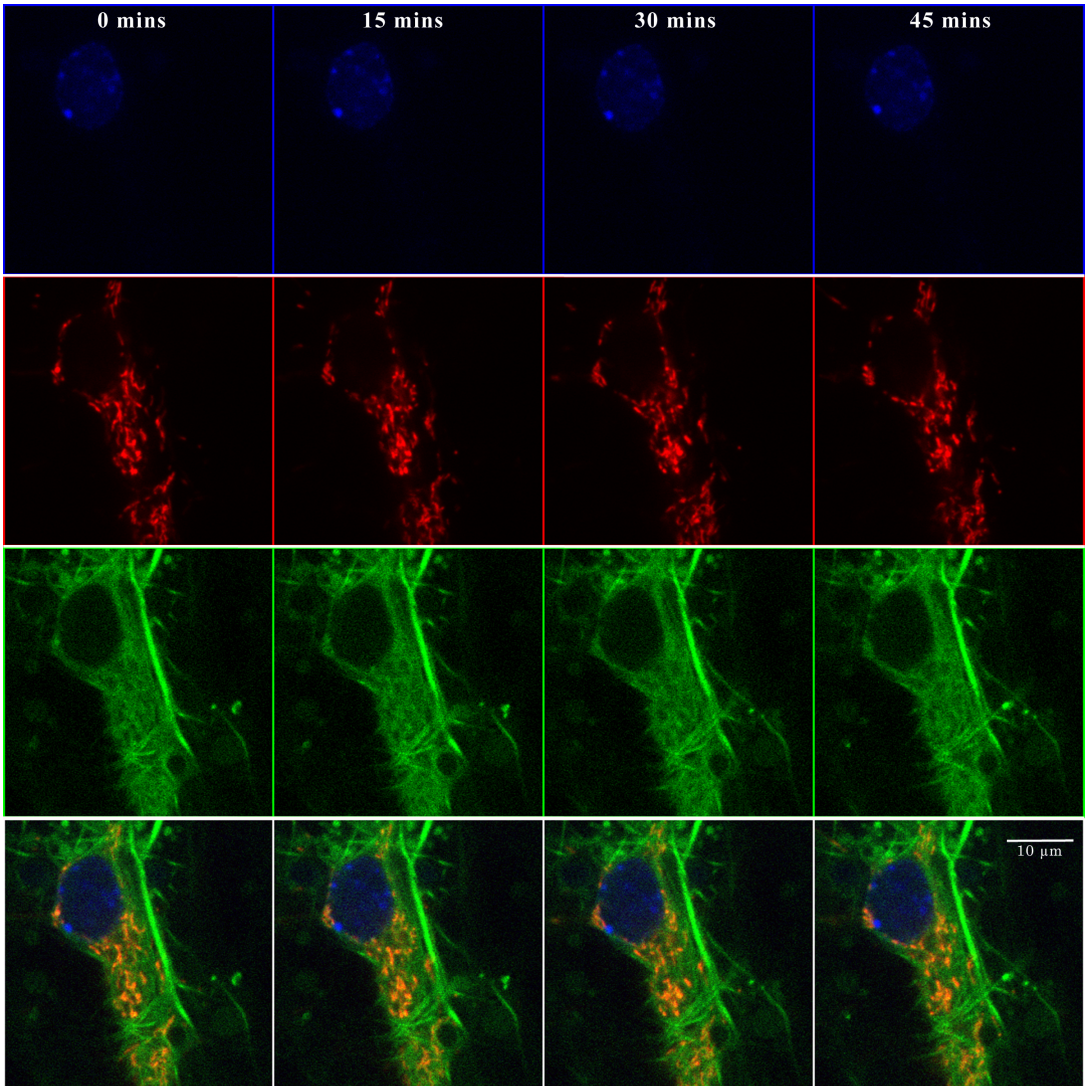

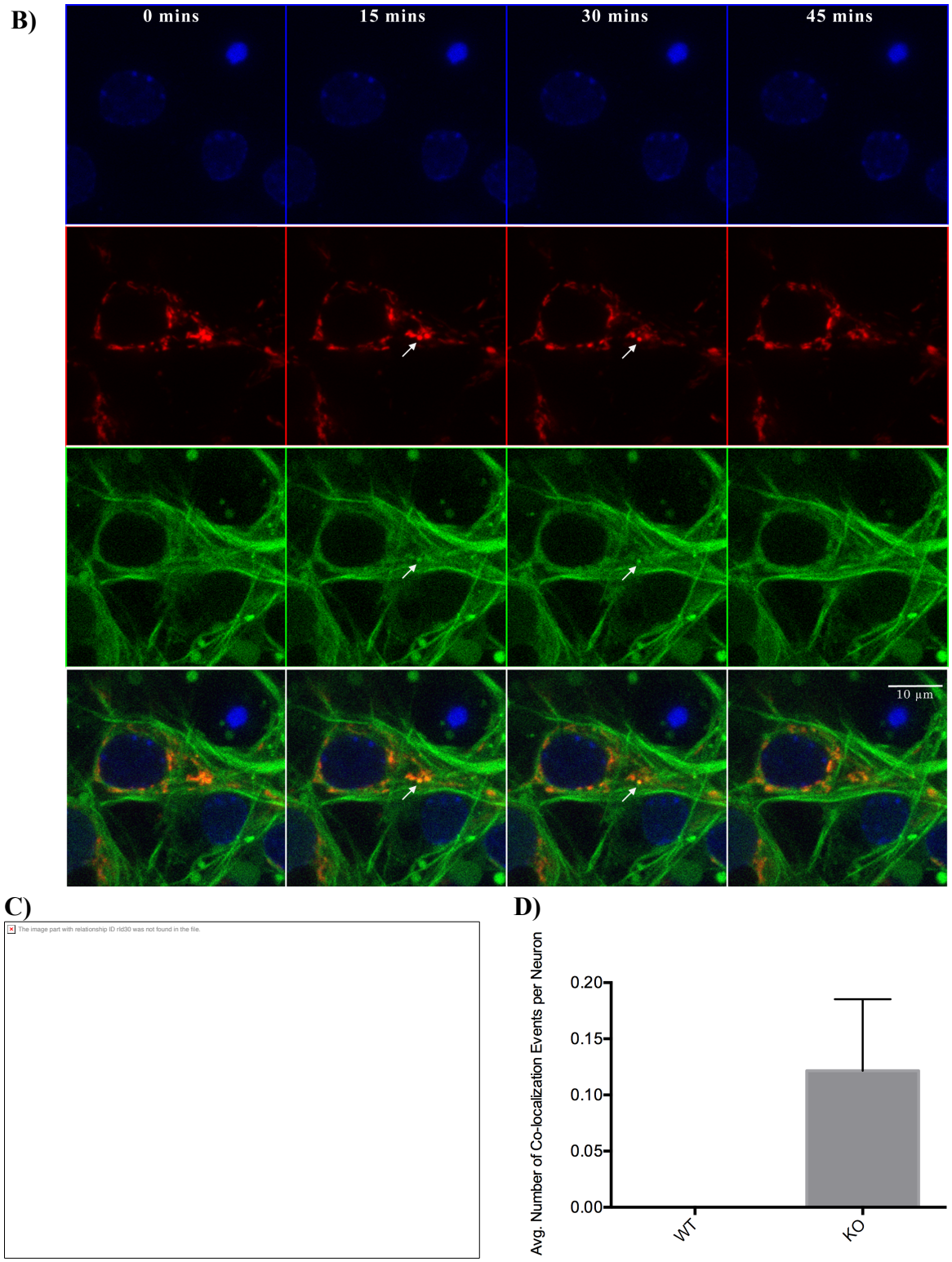

Figure 16. Time-lapse imaging of active mitophagy in live double-transgenic GFP-LC3/AFG3L2 WT and KO murine primary cortical neurons. Time-lapse images of A) WT and B) KO primary cortical neurons presented have been cropped to emphasize region of interest. Labels include nucleus labeled by Hoechst (Blue), OCT-DsRed Expression labeling mitochondria (Red), and endogenous LC3-GFP expression (Green). C) Data

transformed to fraction of total co-labeled neurons with observable co-localization events. N = 121.

5.5 Mitochondrially targeted recombinant PINK1 fragments rescue MEF mitochondrial morphology from AFG3L2 deficiency

To examine how PINK1 cleavage may functionally rescue mitochondrial morphology, we generated recombinant fusion constructs of mitochondrially targeted PINK1-HA fragments that could be expressed in AFG3L2 null MEFs. In this process, the first 35aa of WT PINK1, representing the MTS, were fused to 2 PINK1 fragments, with full-length WT PINK1-HA used as control. These included a Δ104-PINK1-HA representing PARL cleavage at position 103 and a hypothetical PINK1 cleavage fragment of Δ154-PINK1-HA, containing only the kinase and c-terminal domain (Deas et al., 2011). AFG3L2 WT and KO MEFs were used to examine the effect of PINK1 fragments' expression upon mitochondria. This investigation revealed a significant effect of increasing mitochondrial length and mitochondrial networking in mitochondrially targeted cleavage fragment expression compared to full-length PINK1 and vector controls (Figure 17A-B). This result suggests that PINK1 fragments, mimicking endogenous cleavage within the mitochondria that is partially governed by AFG3L2, can overcome deficits associated with AFG3L2 loss through their novel function of regulating mitochondrial morphology.

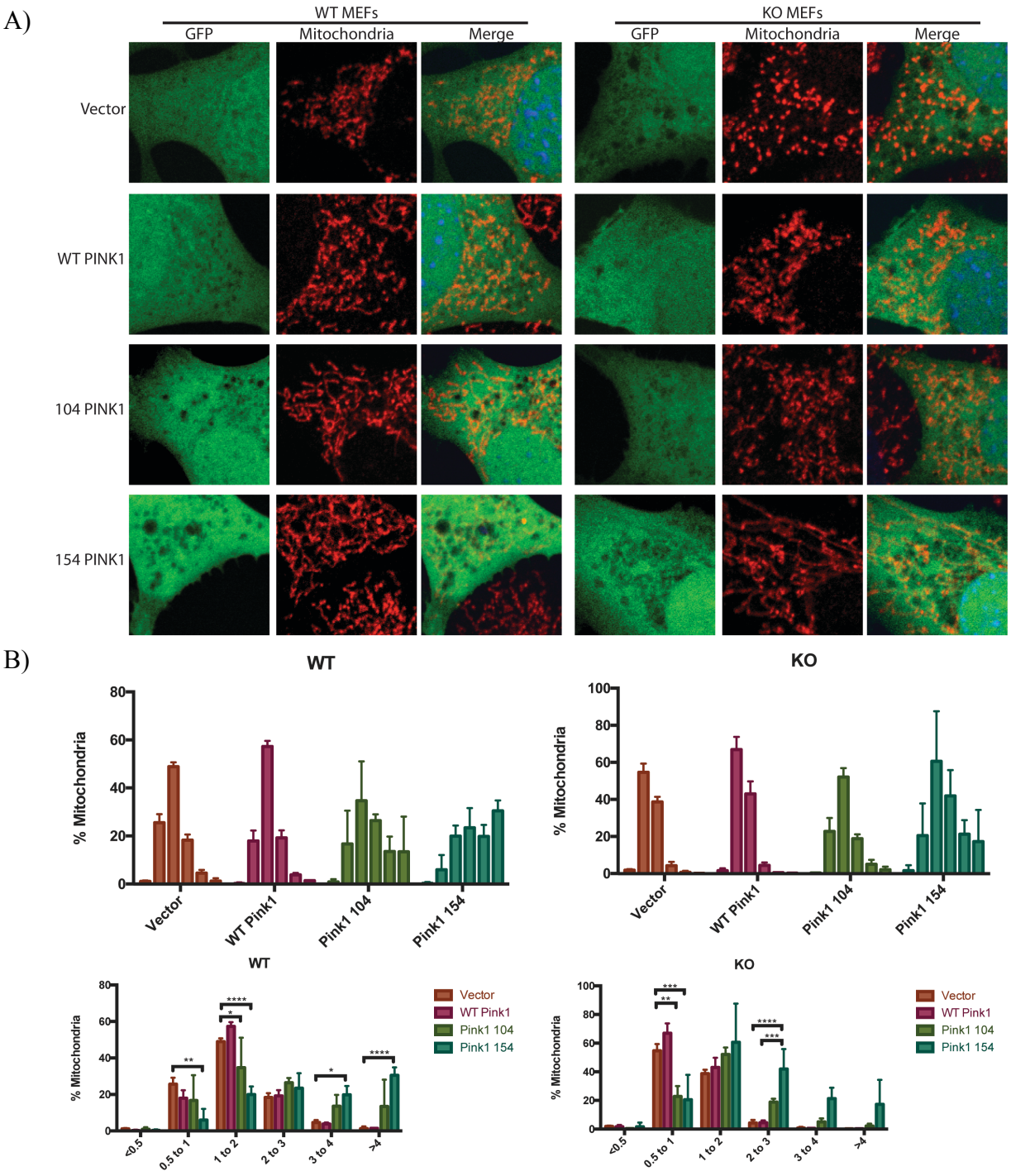

Figure 17. Expression of mitochondrially targeted recombinant PINK1-HA fragments in AFG3L2 WT and KO MEFs upon mitochondrial length. A) MEFs were transfected by Lipofectamine 2000 with plasmid constructs containing WT PINK1, Δ104-PINK1 or Δ154-PINK1, with empty vector used as control. Cells were fixed after 36hrs of expression by 3.7% formalin and mitochondria were labelled by anti-MTCO1. Positively transfected cells examined were identified by vector GFP expression. B) Statistical analysis of mitochondrial length was calculated by two-way ANOVA F (15, 48) with significance represented by Tukeys multiple comparisons. Data collected and analysed by Joselin *et al.* N = 250.

DISCUSSION

PD is the most common of the movement neurodegenerative disorders, with no current treatment options that can to slow or reverse the progress of the disease. Our study begins to examine the molecular mechanisms by which PD pathogenesis manifests through better understanding the function of proteins linked to PD onset.

PINK1 has also been examined extensively under similar oxidative stress conditions. Under these circumstances PINK1 has been shown to respond to mitochondrial damage mediated by toxic insult of CCCP, an agent that facilitates depolarization of the mitochondrial membrane. Here PINK1 binds to the TOM7 complex, phosphorylates ubiquitin, and assists in initiating the cascade of Parkin recruitment and mitochondrial clearance via mitophagy (Hasson et al., 2013; Kane et al., 2014). However, although under mitochondrial stress PINK1 is well understood, PINK1's endogenous functions, when healthy mitochondria are present, has been examined less extensively. In only one study using a PINK1-F104A mutant inhibiting PARL's cleavage, PINK1 expression resulted in the accumulation of N-terminal deletion of PINK1 within the mitochondria, leading to increased basal mitochondrial membrane potential (Deas et al., 2011). As well, if processing is solely part of PINK1 degradation, PD-linked mutations such as PINK1-C92F occurring within a known cleaved-off region become difficult to associate with PINK1 dysfunction as a part of PD pathogenesis (Haque et al., 2008; Okatsu et al., 2013; Valente et al., 2004).

DJ-1 has been examined extensively by both *in vitro* and *in-vivo* models. Through this analysis DJ-1 has primarily been linked to respond to oxidative stress, where previous studies examining DJ-1 deficiency have demonstrated an increase sensitization to oxidative stress following H_2O_2 treatment *in vitro* and MPTP *in-vivo* (Aleyasin et al.,

2010; R. Kim et al., 2005). However, although we have gained a better understanding of DJ-1's protective effects against oxidative stress, these results do not explain the evidence of DJ-1's association with increased autophagic flux. In this thesis, we attempt to better understand the mechanism by which DJ-1 and PINK1 function from identifying their protein interactors by Co-IP mass spectroscopy in collaboration with Dr. Daniel Figeys (Ewing et al., 2007). By this means we identified protein interaction candidates for both DJ-1 and PINK1. For DJ-1, we identified ATG5 and ATG12 as potential protein interactors. For PINK1 we identified AFG3L2 as a potential protein interactor; an interaction that was successfully verified through Co-IP of their over-expressed recombinant proteins PINK1-Flag and AFG3L2-myc.

ASSESSING THE INTERACTION OF DJ-1 WITH AUTOPHAGY RELATED PROTEINS ATG5 AND ATG12

Co-Immunoprecipitation of DJ-1, ATG5 and ATG12

Before attempting to understand the functional interaction of DJ-1 with autophagy, potentially mediated by ATG5 or ATG12, it was important to verify the mass spectroscopy result indicating ATG5 and ATG12 directly interact with DJ-1. The mass spectroscopy screen was conducted by identifying the Co-IP proteins of DJ-1 expression in HEK293 cells (Ewing et al., 2007). Other interaction candidates Paraxonase-2 (PON2) and VHL from the screen have also been verified indicating the screens ability to identify confirmable targets (Parsanejad, Bourquard, et al., 2014a; Parsanejad, Zhang, et al., 2014b). The interaction was tested by Co-IP through multiple methodologies using HEK293 cells. Our initial hypothesis would suggest that DJ-1 would interact with ATG5-

ATG12 in order to inhibit autophagy, with DJ-1 loss resulting in increased autophagic flux (Irrcher et al., 2010). We found no interaction following over-expression of each protein (Figure 4-5), in naïve or autophagy induced conditions, induced by starvation. In addition, as endogenously ATG5-ATG12 are primarily found conjugated, thus expressing both parties would likely increase the conjugate and therefore potentially increase the likelihood of interaction with DJ-1 (Kuma, Mizushima, Ishihara, & Ohsumi, 2002). However under these conditions, we could not co-immunoprecipitate DJ-1 (Figure 5). To overcome possible interaction limitations based on total protein levels, we attempted overexpression of all three ATG5, ATG12 and DJ-1 (Figure 6). Varying lysis detergent concentration were also checked as they are known to impact protein interaction as well (Antrobus & Borner, 2011; Takahashi, 2015). However our examinations could not elucidate an interaction of DJ-1 with ATG5 and ATG12. Additionally experiments using anti-flag IP and expression in HEK293 cells, resulted in non-specific pull-down of ATG5 and ATG12 occurred in control IP samples, leading to inconclusive results (Figure 8). This may be due to less stringent lysis and wash buffer conditions, which contained 0% detergents, even with lysate pre-clearing prior to antibody incubation (Antrobus & Borner, 2011; Huang & Kim, 2013; "Immunoprecipitation protocol | Abcam," n.d.).

Since these attempts to recapitulate the mass-spectrometry screen in cell culture models were negative or inconclusive, we tested endogenous protein levels from brain samples, which are likely more relevant to PD, as per our previous publications (Qu et al., 2007). Therefore using these conditions, we attempted to perform the Co-IP using age-matched WT and DJ-1 KO whole murine brain extracts. With the IP for endogenous DJ-1, however non-specific pulldown was still observed after pre-clearing lysates, when

probing for endogenous ATG5 or ATG5-ATG12 resulting in inconclusive results (Figure 9). Taking these results as a whole, using both human and mouse cells, over-expression, whole brain extracts and starvation mediated induction of autophagy, our data would suggest that DJ-1 does not appear to directly interact with ATG5 or ATG12. This would indicate the mass spectrometry results identifying ATG5 and ATG12 as interaction candidates may have been a non-specific hit. Our results also hints this is possible as suggested by the inconclusive co-immunoprecipitation of ATG5 and ATG12 occurring after pre-clearing.

Multiple methodologies exist in order to identify direct protein-protein interactions, especially those interactions that can occur in low abundance. One method is chemical cross-linking protein complexes during antibody incubation, as was previously used to identify transient AKT protein interactors (Huang & Kim, 2013). This may be one method that could elucidate a DJ-1, ATG5 and ATG12 interaction. Another is through the use of GST-tagged protein pull-down, previously shown to work with DJ-1 interacting protein PON2 (Parsanejad, Bourquard, et al., 2014a).

DJ-1 may also not interact with ATG5 or ATG12 directly, but may still interact with the autophagy machinery indirectly, leading to its deficiency mediating increased in autophagy flux. One hypothesis would be DJ-1 is involved in bioenergetic homeostasis, functioning by its interaction with the mitochondria and AKT. Recent studies examining DJ-1 function have demonstrated DJ-1's translocation to the mitochondria upon oxidative stress and localization to the mitochondrial matrix upon nutrient deprivation enhancing ATP and decreasing autophagic flux (Calì, Ottolini, Soriano, & Brini, 2015; Joselin et al., 2012). It's expression, previously showing neuroprotective effects, has also been

implicated in increased activated AKT by S473 phosphorylation as well as mTOR independent decreased autophagy (Aleyasin et al., 2010; Huang & Kim, 2013; Jaramillo-Gómez, Niño, Arboleda, & Arboleda, 2015). And taking into account our studies suggesting DJ-1 deficiency leads to mitochondrial fragmentation, increased ROS, and decreased complex 1 activity, this could suggest the effects of DJ-1 may be mediated by the metabolic pathway (Hayashi et al., 2009; Heo et al., 2012; Irrcher et al., 2010). In this pathway, loss of DJ-1 function could result in decreased energy output, resulting indirectly in the increase of starvation mediated autophagy mechanisms. These studies could be the topic of future studies that examine the functional mechanism by which DJ-1 loss facilitates the observed increase in autophagic flux.

UNDERSTANDING PINK1'S FUNCTIONAL INTERACTION WITH MITOCHONDRIAL M-AAA PROTEASE AFG3L2

AFG3L2 mediates PINK1 Cleavage and Stability

As PINK1 was previously identified to interact with AFG3L2 (Joselin *et al.*, unpublished) it was important to examine how the interaction of AFG3L2 may impact PINK1. Therefore using conditions previously established for MPP, also an m-AAA protease, we conducted an *in vitro* assay using a mitochondria-enriched fraction isolated by sub-cellular fractionation as our source for AFG3L2 (Nolden et al., 2005). Through this method we excitingly found that AFG3L2 WT mediated differential cleavage of PINK1-Flag *in vitro* generating an approximately 35kd product not present in KO samples (Figure 12). However AFG3L2 has previously been reported to be involved in PINK1 cleavage regulation as siRNA knockdown of AFG3L2 in HEK293T cells leads to

the accumulation of full-length and MPP-cleaved PINK1 (Greene et al., 2012). Our examination using isolated mitochondria allows for a direct assessment of AFG3L2's functional impact on PINK1 cleavage. In addition, our methodology also allows for examination of PINK1 cleavage without loss of cleaved PINK1 to cellular degradation mechanisms, or importantly the requirement for mitochondrial PINK1 import (Becker et al., 2012; Lin & Kang, 2008). Therefore, although we do not employ purified AFG3L2 complexes, our data does suggests AFG3L2 directly regulates PINK1 cleavage, if we take into account two factors: (i) AFG3L2's interaction with PINK1, and (ii) that its functional complex partner paraplegin, still present in the AFG3L2 KO mitochondria, does not lead to PINK1 cleavage.

The removal of AFG3L2 results in decreased PINK1 cleavage, but leads to decreased total PINK1 protein levels (Figure 11). Interestingly, AAA proteases such as AFG3L2 are also known to have functional chaperone-like activity that may mediate PINK1 stabilization at the mitochondria. This has previously been show with the AAA protease homologs in yeast, the YTA10-12 complex, demonstrating chaperone activity in the formation of ATP synthase (Arlt et al., 1996). More recently, AFG3L2 and paraplegin have also shown chaperone-like function to facilitate the proper formation of Complex I (Luigia Atorino, 2003).

However, our examination is partly in contrast with previously published studies which illustrates the accumulation of PINK1 with AFG3L2 knockdown in HEK293 cells (Greene et al., 2012). It is possible that this may due to species variation, as AFG3L1, a homolog of paraplegin expressed in mice, is not translated in humans (Kremmidiotis et al., 2001). Therefore one possible mechanism resulting in decreased PINK1 stability in

murine cells may be AFG3L1 functioning similarly to paraplegin, and partially compensating for AFG3L2 loss, as evident by its localization and homology (Kremmidiotis et al., 2001). This could allow on average more healthy mitochondria, enabling PINK1 import and partial processing by proteases such as PARL, and ultimately increased degradation by the proteasome upon export (Deas et al., 2011; Lin & Kang, 2008; Sekine et al., 2012). In contrast, loss of AFG3L2 in human cells may be more pronounced, with reduced mitochondrial import allowing for the accumulation of full-length PINK1, avoiding proteasome-mediated degradation, and triggering mitochondrial clearance. To test this hypothesis, AFG3L1 function, mitochondrial function under AFG3L1 loss, and PINK1 localization under AFG3L2 null human and murine cells would need to be examined to better understand the variation between species. Furthermore, as results from both species demonstrate conflicting evidence of PINK1 stability under a cellular model of AFG3L2 loss, assessing chaperone-like regulation of PINK1 stability by AFG3L2 may be undetectable within the context of AFG3L2 loss itself.

Therefore similar to our examination of PINK1 cleavage, through an *in vitro* analysis, we observed if purified human recombinant AFG3L2-GST may also facilitate purified human PINK1-Flag stability using similar conditions to our cleavage assay. We saw that PINK1-flag was successively stabilized with AFG3L2-GST compared to our 80ng GST protein controls (Figure 13). Although we do not completely eliminate known protein-protein stabilization effects (Bajaj & Pande, 2014; Chang & Mahoney, 1995), this would suggest AFG3L2 may not only be involved in PINK1 cleavage regulation, but may also partially regulate PINK1 levels within the mitochondria, regulating its basal activity

AFG3L2 deficiency leads to significantly increased mitochondrial damage and mitophagic flux

As earlier studies, including our own data, show AFG3L2 null murine neurons (Figure 15A), and MEFs exhibiting mitochondrial fragmentation and decreased mitochondrial function, we began to assess if this also may be lead to increased endogenous mitophagy (Almajan et al., 2012; Maltecca et al., 2012). Previous studies examining PINK1-Parkin mediated mitophagy had often shown induction by triggering mitochondrial damage through exogenous treatment with CCCP or by inducing localized damage through irradiation (Ashrafi, Schlehe, LaVoie, & Schwarz, 2014; Jin et al., 2010; Narendra et al., 2008; 2010). Therefore, to examine endogenous mitophagy, AFG3L2 KO MEFs confirmed previously to recapitulate the endogenous mitochondrial fragmentation phenotype, would likely provide an ideal model. With experimental analysis conducted by Joselin *et al.*, we were able to show that indeed endogenous mitochondrial damage by AFG3L2 loss over a 4hr period lead to significantly increased mitophagy when compared to WT controls (Figure 14). This would suggest AFG3L2 loss may represent a model system to examine endogenous mitochondrial damage and mitophagy, that could not only be mediated by loss of PINK1 processing, but present us a means to rescue mitochondrial deficits by PINK1 fragment expression.

To confirm the relevance of AFG3L2 loss within a more PD relevant cellular system, we also needed examine active mitophagy in neuronal cells. Therefore we generated an AFG3L2--GFP-LC3 double-transgenic mouse line. This would enable us to examine endogenous mitophagy using live-cell imaging in cortical neurons, looking for

co-localization of punctate GFP-LC3 structures with mitochondria labelled by lenti-viral expression of OCT-DsRed.

Through this process of live imaging, we successfully observed active mitochondrial clearance in AFG3L2 KO cells as mitochondria undergo co-localization with GFP-LC3 and clear over a 30-45 min period (Figure 16B). With an observed increase in the fraction of cells undergoing mitophagy (Figure 16C) and an increased number of co-localization events in AFG3L2 KO neurons (Figure 16D), although our data cannot be examined statistically, it suggests that loss of AFG3L2 may result in increased mitophagic flux, a pathway directly mediated by PINK1 and Parkin activity. In considering previous studies suggesting loss of AFG3L2 does not lead to a decreased mitochondrial membrane potential that could directly hinder PINK1 import, our data would also suggest that loss of PINK1 processing may play a major role in increased mitochondrial clearance (Maltecca et al., 2012). As a result, AFG3L2 deficiency may represent an ideal model to study the effects of PINK1 processing on endogenous mitochondrial damage with it resulting in increased mitochondrial fragmentation and clearance within both MEFs and cortical neurons. As we have shown AFG3L2 to interact with PINK1 in addition to mediating both its cleavage and stabilization, it enables us to study how cleaved PINK1 may function endogenously after proteolytic cleavage.

Mitochondrially targeted recombinant PINK1 fragments rescue AFG3L2 mediated mitochondrial fragmentation

Up to this point, observations have taken place with respect to AFG3L2's affect upon PINK1 and mitophagy. However, we have not directly examined how PINK1

cleavage, partially mediated by AFG3L2, may play a role within the cell and in particular regulating mitochondrial integrity.

Therefore, we generated novel PINK1 recombinant constructs that may mimic PINK1's effect upon mitochondria by creating PINK1 N-terminal deletion fragments fused to the first 35aa of the WT PINK representing the MTS, shown previously to be minimally required for successful mitochondrial targeting and import (Becker et al., 2012). Of the 2 fragments generated, the MTS-Δ104-PINK-HA would mimic PARL cleavage of PINK1, and the MTS-Δ154-PINK-HA would hypothetically represent the 5th major PINK1 cleavage fragment illustrated in Figure 12, at a predicted weight of 46kd, and theoretical PINK1 cleavage substrate of AFG3L2. In contrast to previously examined N-terminal deletions of PINK1, including our own examinations *in vitro*, mitochondrial targeting was not maintained (Haque et al., 2008). Therefore although cytosolic PINK1 has been shown to provide protection against oxidative stress, and repress Parkin function, PINK1 fragments within the mitochondria where proteolytic cleavage takes place have not been extensively examined (Fedorowicz et al., 2014; Haque et al., 2008). To date only one previous study, which identified PINK1 cleavage by PARL, demonstrated ΔN-PINK1 function within the mitochondria showing increased mitochondrial membrane potential in SH-SY5Y cells (Deas et al., 2011).

Thus we used the approach of mitochondrially targeted recombinant PINK1 fragments to examine the direct effect PINK1 may have upon mitochondrial integrity, with experiments conducted by Joselin *et al.* Through this process we successful observed PINK1-HA fragments performing the novel function of significantly rescuing mitochondrial fragmentation in AFG3L2 KO MEFs compared to vector, or full length

WT PINK1 expression. In addition, not only did mitochondrial length increased, but increased mitochondria networking, an indication of mitochondrial fusion, was also observed (Karbowski & Youle, 2003). However, comparisons between Δ104-PINK1 and Δ154-PINK1 expression upon mitochondrial length were not statistically significant.

The identification of this novel function of PINK1 is important as previous examination of AFG3L2 loss had suggested mitochondrial fragmentation is mediated by altered OPA1 processing resulting in impaired mitochondrial Ca^{2+} homeostasis (Maltecca et al., 2012). Our evidence suggests that endogenous PINK1 cleavage within the mitochondria may also perform a similar function in basally regulating mitochondrial morphology and integrity. Therefore with loss of basal PINK1 processing, mitochondrial function and integrity may be compromised. However, further investigation with PINK1 fragment expression on mitochondrial function, such as by assessing ATP levels, Ca^{2+} levels, and membrane potential, would need to be examined to confirm this effect. In addition, identification of an AFG3L2 directly mediated PINK1 cleavage fragment could also be examined to explore that fragment's function upon mitochondrial integrity.

Conclusion

In conclusion, we have shown that DJ-1, ATG5 and ATG12 do not appear to directly interact. However, this does not rule out DJ-1's influence on autophagic flux indirectly as multiple literature sources would suggest. In addition, we have also demonstrated AFG3L2 to function in regulating both PINK1 processing and stability *in vitro*, indicating its potential role in mediating PINK1 basal activity. We have shown that with endogenous mitochondrial damage by AFG3L2 loss, an increase in mitophagy can

be observed suggesting the role of the PINK1-Parkin pathway potentially in response to loss of proper PINK1 processing. Furthermore, we have elucidated a novel function for PINK1 cleavage fragments at the mitochondria. With mitochondrially targeted PINK1 fragments' expression allowing for the rescue of fragmented AFG3L2 KO mitochondria and increasing both mitochondrial length and mitochondrial networking. These findings suggest PINK1 processing may play a major role in the regulation of mitochondrial function and integrity and provide a better understanding of PINK1's role in the pathogenesis of PD.

REFERENCES

Ahmed, I., Liang, Y., Schools, S., Dawson, V. L., Dawson, T. M., & Savitt, J. M. (2012). Development and characterization of a new Parkinson's disease model resulting from impaired autophagy. *The Journal of Neuroscience : the Official Journal of the Society for Neuroscience*, *32*(46), 16503–16509. http://doi.org/10.1523/JNEUROSCI.0209-12.2012

Aleyasin, H., Rousseaux, M. W. C., Marcogliese, P. C., Hewitt, S. J., Irrcher, I., Joselin, A. P., et al. (2010). DJ-1 protects the nigrostriatal axis from the neurotoxin MPTP by modulation of the AKT pathway. *Proceedings of the National Academy of Sciences*, *107*(7), 3186–3191. http://doi.org/10.1073/pnas.0914876107

Almajan, E. R., Richter, R., Paeger, L., Martinelli, P., Barth, E., Decker, T., et al. (2012). AFG3L2 supports mitochondrial protein synthesis and Purkinje cell survival. *Journal of Clinical Investigation*. http://doi.org/10.1172/JCI64604DS1

Antonini, A., Martinez-Martin, P., Chaudhuri, R. K., Merello, M., Hauser, R., Katzenschlager, R., et al. (2011). Wearing-off scales in Parkinson's disease: critique and recommendations. *Movement Disorders*, *26*(12), 2169–2175. http://doi.org/10.1002/mds.23875

Antrobus, R., & Borner, G. H. H. (2011). Improved elution conditions for native co-immunoprecipitation. *PLoS ONE*, *6*(3), e18218. http://doi.org/10.1371/journal.pone.0018218

Arlt, H., Tauer, R., Feldmann, H., Neupert, W., & Langer, T. (1996). The YTA10-12 complex, an AAA protease with chaperone-like activity in the inner membrane of mitochondria. *Cell*, *85*(6), 875–885.

Ashrafi, G., & Schwarz, T. L. (2012). The pathways of mitophagy for quality control and clearance of mitochondria. *Cell Death and Differentiation*, –. http://doi.org/10.1038/cdd.2012.81

Ashrafi, G., Schlehe, J. S., LaVoie, M. J., & Schwarz, T. L. (2014). Mitophagy of damaged mitochondria occurs locally in distal neuronal axons and requires PINK1 and Parkin. *The Journal of Cell Biology*, *206*(5), 655–670. http://doi.org/10.1083/jcb.201401070

Bajaj, P., & Pande, A. H. (2014). Stabilization Studies on Bacterially Produced Human Paraoxonase 1 for Improving Its Shelf Life. *Applied Biochemistry and Biotechnology*, *172*(8), 3798–3809. http://doi.org/10.1007/s12010-014-0806-5

Becker, D., Richter, J., Tocilescu, M. A., Przedborski, S., & Voos, W. (2012). Pink1 kinase and its membrane potential (Deltaψ)-dependent cleavage product both localize to outer mitochondrial membrane by unique targeting mode. *Journal of Biological Chemistry*, *287*(27), 22969–22987. http://doi.org/10.1074/jbc.M112.365700

Bonifati, V., Rizzu, P., van Baren, M. J., Schaap, O., Breedveld, G. J., Krieger, E., et al. (2003). Mutations in the DJ-1 gene associated with autosomal recessive early-onset parkinsonism. *Science (New York, N.Y.)*, *299*(5604), 256–259. http://doi.org/10.1126/science.1077209

Burbulla, L. F., & Krüger, R. (2011). Converging environmental and genetic pathways in the pathogenesis of Parkinson's disease. *Journal of the Neurological Sciences*, *306*(1-2), 1–8. http://doi.org/10.1016/j.jns.2011.04.005

Cai, Q., Zakaria, H. M., Simone, A., & Sheng, Z.-H. (2012). Spatial parkin translocation

and degradation of damaged mitochondria via mitophagy in live cortical neurons. *Current Biology : CB*, *22*(6), 545–552. http://doi.org/10.1016/j.cub.2012.02.005

Calì, T., Ottolini, D., Soriano, M. E., & Brini, M. (2015). A new split-GFP-based probe reveals DJ-1 translocation into the mitochondrial matrix to sustain ATP synthesis upon nutrient deprivation. *Human Molecular Genetics*, *24*(4), 1045–1060. http://doi.org/10.1093/hmg/ddu519

Canada, P. S. (2012, January). Parkinson Society Canada Fact Sheet - March 2012. Retrieved March 8, 2016, from http://www.parkinson.ca/atf/cf/%7B9ebd08a9-7886-4b2d-a1c4-a131e7096bf8%7D/PARKINSON_SOCIETY_CANADA_FACT%20SHEET%20MARCH%202012.PDF

Canet-Avilés, R. M., Wilson, M. A., Miller, D. W., Ahmad, R., McLendon, C., Bandyopadhyay, S., et al. (2004). The Parkinson's disease protein DJ-1 is neuroprotective due to cysteine-sulfinic acid-driven mitochondrial localization. *Proceedings of the National Academy of Sciences of the United States of America*, *101*(24), 9103–9108. http://doi.org/10.1073/pnas.0402959101

Chang, B. S., & Mahoney, R. R. (1995). Enzyme thermostabilization by bovine serum albumin and other proteins: evidence for hydrophobic interactions. *Biotechnology and Applied Biochemistry*, *22 (Pt 2)*(2), 203–214. http://doi.org/10.1111/j.1470-8744.1995.tb00346.x

Choi, I., Kim, J., Jeong, H.-K., Kim, B., Jou, I., Park, S. M., et al. (2013). PINK1 deficiency attenuates astrocyte proliferation through mitochondrial dysfunction, reduced AKT and increased p38 MAPK activation, and downregulation of EGFR. *Glia*, *61*(5), 800–812. http://doi.org/10.1002/glia.22475

Cookson, M. R. (2010). The role of leucine-rich repeat kinase 2 (LRRK2) in Parkinson's disease. *Nature Reviews. Neuroscience*, *11*(12), 791–797. http://doi.org/10.1038/nrn2935

Dauer, W., & Przedborski, S. (2003). Parkinson's disease: mechanisms and models. *Neuron*, *39*(6), 889–909.

Deas, E., Plun-Favreau, H., Gandhi, S., Desmond, H., Kjaer, S., Loh, S. H. Y., et al. (2011). PINK1 cleavage at position A103 by the mitochondrial protease PARL. *Human Molecular Genetics*, *20*(5), 867–879. http://doi.org/10.1093/hmg/ddq526

Dexter, D. T., & Jenner, P. (2013). Parkinson disease: from pathology to molecular disease mechanisms. *Free Radical Biology & Medicine*, *62*, 132–144. http://doi.org/10.1016/j.freeradbiomed.2013.01.018

Ehses, S., Raschke, I., Mancuso, G., Bernacchia, A., Geimer, S., Tondera, D., et al. (2009). Regulation of OPA1 processing and mitochondrial fusion by m-AAA protease isoenzymes and OMA1. *The Journal of Cell Biology*, *187*(7), 1023–1036. http://doi.org/10.1083/jcb.200906084

Ewing, R. M., Chu, P., Elisma, F., Li, H., Taylor, P., Climie, S., et al. (2007). Large-scale mapping of human protein-protein interactions by mass spectrometry. *Molecular Systems Biology*, *3*, 89. http://doi.org/10.1038/msb4100134

Fedorowicz, M. A., de Vries-Schneider, R. L. A., Rüb, C., Becker, D., Huang, Y., Zhou, C., et al. (2014). Cytosolic cleaved PINK1 represses Parkin translocation to mitochondria and mitophagy. *EMBO Reports*, *15*(1), 86–93. http://doi.org/10.1002/embr.201337294

Gong, X., Tang, X., Wiedmann, M., Wang, X., Peng, J., Zheng, D., et al. (2003). Cdk5-mediated inhibition of the protective effects of transcription factor MEF2 in neurotoxicity-induced apoptosis. *Neuron*, *38*(1), 33–46.

González, P., Alvarez, V., Menéndez, M., Lahoz, C. H., Martínez, C., Corao, A. I., et al. (2007). Myocyte enhancing factor-2A in Alzheimer's disease: genetic analysis and association with MEF2A-polymorphisms. *Neuroscience Letters*, *411*(1), 47–51. http://doi.org/10.1016/j.neulet.2006.09.055

Greene, A. W., Grenier, K., Aguileta, M. A., Muise, S., Farazifard, R., Haque, M. E., et al. (2012). Mitochondrial processing peptidase regulates PINK1 processing, import and Parkin recruitment. *EMBO Reports*, *13*(4), 378–385. http://doi.org/10.1038/embor.2012.14

Haehner, A., Hummel, T., & Reichmann, H. (2011). Olfactory loss in Parkinson's disease. *Parkinson's Disease*, *2011*, 450939. http://doi.org/10.4061/2011/450939

Hanada, T., Noda, N. N., Satomi, Y., Ichimura, Y., Fujioka, Y., Takao, T., et al. (2007). The Atg12-Atg5 conjugate has a novel E3-like activity for protein lipidation in autophagy. *The Journal of Biological Chemistry*, *282*(52), 37298–37302. http://doi.org/10.1074/jbc.C700195200

Haque, M. E., Mount, M. P., Safarpour, F., Abdel-Messih, E., Callaghan, S., Mazerolle, C., et al. (2012). Inactivation of Pink1 gene in vivo sensitizes dopamine-producing neurons to 1-methyl-4-phenyl-1,2,3,6-tetrahydropyridine (MPTP) and can be rescued by autosomal recessive Parkinson disease genes, Parkin or DJ-1. *Journal of Biological Chemistry*, *287*(27), 23162–23170. http://doi.org/10.1074/jbc.M112.346437

Haque, M. E., Thomas, K. J., D'Souza, C., Callaghan, S., Kitada, T., Slack, R. S., et al. (2008). Cytoplasmic Pink1 activity protects neurons from dopaminergic neurotoxin MPTP. *Proceedings of the National Academy of Sciences*, *105*(5), 1716–1721. http://doi.org/10.1073/pnas.0705363105

Harris, H., & Rubinsztein, D. C. (2011). Control of autophagy as a therapy for neurodegenerative disease. *Nature Reviews. Neurology*. http://doi.org/10.1038/nrneurol.2011.200

Hasson, S. A., Kane, L. A., Yamano, K., Huang, C.-H., Sliter, D. A., Buehler, E., et al. (2013). High-content genome-wide RNAi screens identify regulators of parkin upstream of mitophagy. *Nature*, *504*(7479), 291–295. http://doi.org/10.1038/nature12748

Hayashi, T., Ishimori, C., Takahashi-Niki, K., Taira, T., Kim, Y.-C., Maita, H., et al. (2009). DJ-1 binds to mitochondrial complex I and maintains its activity. *Biochemical and Biophysical Research Communications*, *390*(3), 667–672. http://doi.org/10.1016/j.bbrc.2009.10.025

Heo, J. Y., Park, J. H., Kim, S. J., Seo, K. S., Han, J. S., Lee, S. H., et al. (2012). DJ-1 null dopaminergic neuronal cells exhibit defects in mitochondrial function and structure: involvement of mitochondrial complex I assembly. *PLoS ONE*, *7*(3), e32629. http://doi.org/10.1371/journal.pone.0032629

Huang, B. X., & Kim, H.-Y. (2013). Effective identification of Akt interacting proteins by two-step chemical crosslinking, co-immunoprecipitation and mass spectrometry. *PLoS ONE*, *8*(4), e61430. http://doi.org/10.1371/journal.pone.0061430

Immunoprecipitation protocol | Abcam. (n.d.). Immunoprecipitation protocol | Abcam.

Retrieved July 13, 2016, from http://www.abcam.com/protocols/immunoprecipitation-protocol-1

Irrcher, I., & Park, D. S. (2009). Parkinson's disease: to live or die by autophagy. *Science Signaling*, *2*(65), pe21. http://doi.org/10.1126/scisignal.265pe21

Irrcher, I., Aleyasin, H., Seifert, E. L., Hewitt, S. J., Chhabra, S., Phillips, M., et al. (2010). Loss of the Parkinson's disease-linked gene DJ-1 perturbs mitochondrial dynamics. *Human Molecular Genetics*, *19*(19), 3734–3746. http://doi.org/10.1093/hmg/ddq288

Jankovic, J. (2008). Parkinson's disease: clinical features and diagnosis. *Journal of Neurology, Neurosurgery, and Psychiatry*, *79*(4), 368–376. http://doi.org/10.1136/jnnp.2007.131045

Jaramillo-Gómez, J., Niño, A., Arboleda, H., & Arboleda, G. (2015). Overexpression of DJ-1 protects against C2-ceramide-induced neuronal death through activation of the PI3K/AKT pathway and inhibition of autophagy. *Neuroscience Letters*, *603*, 71–76. http://doi.org/10.1016/j.neulet.2015.07.032

Jin, S. M., & Youle, R. J. (2013). The accumulation of misfolded proteins in the mitochondrial matrix is sensed by PINK1 to induce PARK2/Parkin-mediated mitophagy of polarized mitochondria. *Autophagy*, *9*(11), 1750–1757. http://doi.org/10.4161/auto.26122

Jin, S. M., Lazarou, M., Wang, C., Kane, L. A., Narendra, D. P., & Youle, R. J. (2010). Mitochondrial membrane potential regulates PINK1 import and proteolytic destabilization by PARL. *The Journal of Cell Biology*, *191*(5), 933–942. http://doi.org/10.1083/jcb.201008084

Joselin, A. P., Hewitt, S. J., Callaghan, S. M., Kim, R. H., Chung, Y.-H., Mak, T. W., et al. (2012). ROS dependent regulation of Parkin and DJ-1 localization during oxidative stress in neurons. *Human Molecular Genetics*. http://doi.org/10.1093/hmg/dds325

Kabeya, Y., Mizushima, N., Uero, T., Yamamoto, A., Kirisako, T., Noda, T., et al. (2000). LC3, a mammalian homologue of yeast Apg8p, is localized in autophagosome membranes after processing. *Embo Journal*, *19*(21), 5720–5728. http://doi.org/10.1093/emboj/19.21.5720

Kane, L. A., Lazarou, M., Fogel, A. I., Li, Y., Yamano, K., Sarraf, S. A., et al. (2014). PINK1 phosphorylates ubiquitin to activate Parkin E3 ubiquitin ligase activity. *The Journal of Cell Biology*, *205*(2), 143–153. http://doi.org/10.1083/jcb.201402104

Karbowski, M., & Youle, R. J. (2003). Dynamics of mitochondrial morphology in healthy cells and during apoptosis. *Cell Death and Differentiation*, *10*(8), 870–880. http://doi.org/10.1038/sj.cdd.4401260

Karbowski, M., & Youle, R. J. (2011). Regulating mitochondrial outer membrane proteins by ubiquitination and proteasomal degradation. *Current Opinion in Cell Biology*, *23*(4), 476–482. http://doi.org/10.1016/j.ceb.2011.05.007

Kim, R., Smith, P., Aleyasin, H., Hayley, S., Mount, M., Pownall, S., et al. (2005). Hypersensitivity of DJ-1-deficient mice to 1-methyl-4-phenyl-1,2,3,6-tetrahydropyrindine (MPTP) and oxidative stress. *Proceedings of the National Academy of Sciences of the United States of America*, *102*(14), 5215–5220. http://doi.org/10.1073/pnas.0501282102

Kitada, T., Asakawa, S., Hattori, N., Matsumine, H., Yamamura, Y., Minoshima, S., et al.

(1998). Mutations in the parkin gene cause autosomal recessive juvenile parkinsonism. *Nature*, *392*(6676), 605–608. http://doi.org/10.1038/33416

Kitada, T., Tong, Y., Gautier, C. A., & Shen, J. (2009). Absence of nigral degeneration in aged parkin/DJ-1/PINK1 triple knockout mice. *Journal of Neurochemistry*, *111*(3), 696–702. http://doi.org/10.1111/j.1471-4159.2009.06350.x

Klionsky, D. J. (2007). Autophagy: from phenomenology to molecular understanding in less than a decade. *Nature Reviews. Molecular Cell Biology*, *8*(11), 931–937. http://doi.org/10.1038/nrm2245

Klionsky, D. J., Abeliovich, H., Agostinis, P., Agrawal, D. K., Aliev, G., Askew, D. S., et al. (2008). Guidelines for the use and interpretation of assays for monitoring autophagy in higher eukaryotes. *Autophagy*, *4*(2), 151–175.

Kremmidiotis, G., Gardner, A. E., Settasatian, C., Savoia, A., Sutherland, G. R., & Callen, D. F. (2001). Molecular and Functional Analyses of the Human and Mouse Genes Encoding AFG3L1, a Mitochondrial Metalloprotease Homologous to the Human Spastic Paraplegia Protein. *Genomics*, *76*(1-3), 58–65. http://doi.org/10.1006/geno.2001.6560

Kuma, A., Mizushima, N., Ishihara, N., & Ohsumi, Y. (2002). Formation of the approximately 350-kDa Apg12-Apg5.Apg16 multimeric complex, mediated by Apg16 oligomerization, is essential for autophagy in yeast. *The Journal of Biological Chemistry*, *277*(21), 18619–18625. http://doi.org/10.1074/jbc.M111889200

Lelos, M. J., Morgan, R. J., Kelly, C. M., Torres, E. M., Rosser, A. E., & Dunnett, S. B. (2016). Amelioration of non-motor dysfunctions after transplantation of human dopamine neurons in a model of Parkinson's disease. *Experimental Neurology*, *278*, 54–61. http://doi.org/10.1016/j.expneurol.2016.02.003

Lim, J., Kim, H.-W., Youdim, M. B. H., Rhyu, I. J., Choe, K.-M., & Oh, Y. J. (2011). Binding preference of p62 towards LC3-ll during dopaminergic neurotoxin-induced impairment of autophagic flux. *Autophagy*, *7*(1), 51–60.

Lin, W., & Kang, U. J. (2008). Characterization of PINK1 processing, stability, and subcellular localization. *Journal of Neurochemistry*, *106*(1), 464–474. http://doi.org/10.1111/j.1471-4159.2008.05398.x

Löbbe, A. M., Kang, J.-S., Hilker, R., Hackstein, H., Müller, U., & Nolte, D. (2013). A Novel Missense Mutation in AFG3L2 Associated with Late Onset and Slow Progression of Spinocerebellar Ataxia Type 28. *Journal of Molecular Neuroscience : MN*. http://doi.org/10.1007/s12031-013-0187-1

Luigia Atorino, L. S. M. K. L. C. A. B. R. M. T. L. G. C. (2003). Loss of m-AAA protease in mitochondria causes complex I deficiency and increased sensitivity to oxidative stress in hereditary spastic paraplegia. *The Journal of Cell Biology*, *163*(4), 777. http://doi.org/10.1083/jcb.200304112

Maltecca, F., Aghaie, A., Schroeder, D. G., Cassina, L., Taylor, B. A., Phillips, S. J., et al. (2008). The mitochondrial protease AFG3L2 is essential for axonal development. *The Journal of Neuroscience : the Official Journal of the Society for Neuroscience*, *28*(11), 2827–2836. http://doi.org/10.1523/JNEUROSCI.4677-07.2008

Maltecca, F., De Stefani, D., Cassina, L., Consolato, F., Wasilewski, M., Scorrano, L., et al. (2012). Respiratory dysfunction by AFG3L2 deficiency causes decreased mitochondrial calcium uptake via organellar network fragmentation. *Human Molecular Genetics*, *21*(17), 3858–3870. http://doi.org/10.1093/hmg/dds214

Mancuso, G. G., Barth, E. E., Pietro P Crivello, & Rugarli, E. I. E. (2012). Alternative splicing of spg7, a gene involved in hereditary spastic paraplegia, encodes a variant of paraplegin targeted to the endoplasmic reticulum. *PLoS ONE*, *7*(5), e36337–e36337. http://doi.org/10.1371/journal.pone.0036337

Mizushima, N., & Komatsu, M. (2011). Autophagy: renovation of cells and tissues. *Cell*, *147*(4), 728–741. http://doi.org/10.1016/j.cell.2011.10.026

Mizushima, N., Levine, B., Cuervo, A. M., & Klionsky, D. J. (2008). Autophagy fights disease through cellular self-digestion. *Nature*, *451*(7182), 1069–1075. http://doi.org/10.1038/nature06639

Mizushima, N., Yamamoto, A., Matsui, M., Yoshimori, T., & Ohsumi, Y. (2004). In vivo analysis of autophagy in response to nutrient starvation using transgenic mice expressing a fluorescent autophagosome marker. *Molecular Biology of the Cell*, *15*(3), 1101–1111. http://doi.org/10.1091/mbc.E03-09-0704

Mizushima, N., Yoshimori, T., & Ohsumi, Y. (2003). Role of the Apg12 conjugation system in mammalian autophagy. *The International Journal of Biochemistry & Cell Biology*, *35*(5), 553–561. http://doi.org/10.1016/S1357-2725(02)00343-6

Mizushima, N., Yoshimori, T., & Ohsumi, Y. (2011). The role of atg proteins in autophagosome formation. *Annual Review of Cell and Developmental Biology*, *27*, 107–132. http://doi.org/10.1146/annurev-cellbio-092910-154005

Moore, D. J., West, A. B., Dawson, V. L., & Dawson, T. M. (2005a). Molecular pathophysiology of Parkinson's disease. *Annual Review of Neuroscience*, *28*, 57–87. http://doi.org/10.1146/annurev.neuro.28.061604.135718

Moore, D. J., Zhang, L., Troncoso, J., Lee, M. K., Hattori, N., Mizuno, Y., et al. (2005b). Association of DJ-1 and parkin mediated by pathogenic DJ-1 mutations and oxidative stress. *Human Molecular Genetics*, *14*(1), 71–84. http://doi.org/10.1093/hmg/ddi007

Morais, V. A., Haddad, D., Craessaerts, K., De Bock, P.-J., Swerts, J., Vilain, S., et al. (2014). PINK1 Loss of Function Mutations Affect Mitochondrial Complex I Activity via NdufA10 Ubiquinone Uncoupling. *Science (New York, N.Y.)*. http://doi.org/10.1126/science.1249161

Morais, V. A., Verstreken, P., Roethig, A., Smet, J., Snellinx, A., Vanbrabant, M., et al. (2009). Parkinson's disease mutations in PINK1 result in decreased Complex I activity and deficient synaptic function. *EMBO Molecular Medicine*, *1*(2), 99–111. http://doi.org/10.1002/emmm.200900006

Narendra, D. P. D., Jin, S. M. S., Tanaka, A. A., Suen, D.-F. D., Gautier, C. A. C., Shen, J. J., et al. (2010). PINK1 is selectively stabilized on impaired mitochondria to activate Parkin. *PLoS Biology*, *8*(1), e1000298–e1000298. http://doi.org/10.1371/journal.pbio.1000298

Narendra, D., Tanaka, A., Suen, D.-F., & Youle, R. J. (2008). Parkin is recruited selectively to impaired mitochondria and promotes their autophagy. *The Journal of Cell Biology*, *183*(5), 795–803. http://doi.org/10.1083/jcb.200809125

Nolden, M., Ehses, S., Koppen, M., Bernacchia, A., Rugarli, E. I., & Langer, T. (2005). The m-AAA protease defective in hereditary spastic paraplegia controls ribosome assembly in mitochondria. *Cell*, *123*(2), 277–289. http://doi.org/10.1016/j.cell.2005.08.003

Okatsu, K., Oka, T., Iguchi, M., Imamura, K., Kosako, H., Tani, N., et al. (2012). PINK1

autophosphorylation upon membrane potential dissipation is essential for Parkin recruitment to damaged mitochondria. *Nature Communications*, *3*, 1016. http://doi.org/10.1038/ncomms2016

Okatsu, K., Uno, M., Koyano, F., Go, E., Kimura, M., Oka, T., et al. (2013). A dimeric PINK1-containing complex on depolarized mitochondria stimulates Parkin recruitment. *Journal of Biological Chemistry*, *288*(51), 36372–36384. http://doi.org/10.1074/jbc.M113.509653

Parkinson, J. (2002). An essay on the shaking palsy. 1817. *The Journal of neuropsychiatry and clinical neurosciences* (Vol. 14, pp. 223–36– discussion 222). http://doi.org/10.1176/jnp.14.2.223

Parsanejad, M., Bourquard, N., Qu, D., Zhang, Y., Huang, E., Rousseaux, M. W. C., et al. (2014a). DJ-1 interacts with and regulates paraoxonase-2, an enzyme critical for neuronal survival in response to oxidative stress. *PLoS ONE*, *9*(9), e106601. http://doi.org/10.1371/journal.pone.0106601

Parsanejad, M., Zhang, Y., Qu, D., Irrcher, I., Rousseaux, M. W. C., Aleyasin, H., et al. (2014b). Regulation of the VHL/HIF-1 pathway by DJ-1. *The Journal of Neuroscience : the Official Journal of the Society for Neuroscience*, *34*(23), 8043–8050. http://doi.org/10.1523/JNEUROSCI.1244-13.2014

Pridgeon, J. W., Olzmann, J. A., Chin, L.-S., & Li, L. (2007). PINK1 protects against oxidative stress by phosphorylating mitochondrial chaperone TRAP1. *PLoS Biology*, *5*(7), e172–e172. http://doi.org/10.1371/journal.pbio.0050172

Qu, D., Rashidian, J., Mount, M. P., Aleyasin, H., Parsanejad, M., Lira, A., et al. (2007). Role of Cdk5-mediated phosphorylation of Prx2 in MPTP toxicity and Parkinson's disease. *Neuron*, *55*(1), 37–52. http://doi.org/10.1016/j.neuron.2007.05.033

Ramaker, C., Marinus, J., Stiggelbout, A. M., & Van Hilten, B. J. (2002). Systematic evaluation of rating scales for impairment and disability in Parkinson's disease. *Movement Disorders*, *17*(5), 867–876. http://doi.org/10.1002/mds.10248

Ramelot, T. A., Yang, Y., Sahu, I. D., Lee, H.-W., Xiao, R., Lorigan, G. A., et al. (2013). NMR structure and MD simulations of the AAA protease intermembrane space domain indicates peripheral membrane localization within the hexaoligomer. *FEBS Letters*. http://doi.org/10.1016/j.febslet.2013.09.009

Reggiori, F., & Klionsky, D. J. (2002). Autophagy in the eukaryotic cell. *Eukaryotic Cell*, *1*(1), 11–21.

Reichmann, H. (2016). Modern treatment in Parkinson's disease, a personal approach. *Journal of Neural Transmission*, *123*(1), 73–80. http://doi.org/10.1007/s00702-015-1441-1

Roh, C. F., Montagna, P., Breedveld, G., Cortelli, P., Oostra, B. A., & Bonifati, V. (2004). Homozygous PINK1 C-terminus mutation causing early-onset parkinsonism. *Annals of Neurology*, *56*(3), 427–431. http://doi.org/10.1002/ana.20247

Rousseaux, M. W. C., Marcogliese, P. C., Qu, D., Hewitt, S. J., Seang, S., Kim, R. H., et al. (n.d.). Progressive dopaminergic cell loss with unilateral-to-bilateral progression in a genetic model of Parkinson disease. http://doi.org/10.1073/pnas.1205102109

Rubinsztein, D. C. (2006). The roles of intracellular protein-degradation pathways in neurodegeneration. *Nature*, *443*(7113), 780–786. http://doi.org/10.1038/nature05291

Schenck, C. H., Bundlie, S. R., & Mahowald, M. W. (1996). Delayed emergence of a parkinsonian disorder in 38% of 29 older men initially diagnosed with idiopathic

rapid eye movement sleep behaviour disorder. *Neurology*, *46*(2), 388–393. http://doi.org/10.1212/WNL.46.2.388

Sekine, S., Kanamaru, Y., Koike, M., Nishihara, A., Okada, M., Kinoshita, H., et al. (2012). Rhomboid Protease PARL Mediates the Mitochondrial Membrane Potential Loss-induced Cleavage of PGAM5. *Journal of Biological Chemistry*, *287*(41), 34635–34645. http://doi.org/10.1074/jbc.M112.357509

Song, S., Jang, S., Park, J., Bang, S., Choi, S., Kwon, K.-Y., et al. (2013). Characterization of PINK1 (PTEN-induced putative kinase 1) mutations associated with Parkinson disease in mammalian cells and Drosophila. *Journal of Biological Chemistry*, *288*(8), 5660–5672. http://doi.org/10.1074/jbc.M112.430801

Sou, Y.-S., Waguri, S., Iwata, J.-I., Ueno, T., Fujimura, T., Hara, T., et al. (2008). The Atg8 Conjugation System Is Indispensable for Proper Development of Autophagic Isolation Membranes in Mice. *Molecular Biology of the Cell*, *19*(11), 4762–4775. http://doi.org/10.1091/mbc.E08-03-0309

Takahashi, Y. (2015). Co-immunoprecipitation from Transfected Cells. In *Protein-Protein Interactions* (Vol. 1278, pp. 381–389). New York, NY: Springer New York. http://doi.org/10.1007/978-1-4939-2425-7_25

Takatori, S., Ito, G., & Iwatsubo, T. (2008). Cytoplasmic localization and proteasomal degradation of N-terminally cleaved form of PINK1. *Neuroscience Letters*, *430*(1), 13–17. http://doi.org/10.1016/j.neulet.2007.10.019

Valente, E. M., Salvi, S., Ialongo, T., Marongiu, R., Elia, A. E., Caputo, V., et al. (2004). PINK1 mutations are associated with sporadic early-onset parkinsonism. *Annals of Neurology*, *56*(3), 336–341. http://doi.org/10.1002/ana.20256

Vincow, E. S., Merrihew, G., Thomas, R. E., Shulman, N. J., Beyer, R. P., Maccoss, M. J., & Pallanck, L. J. (2013). The PINK1-Parkin pathway promotes both mitophagy and selective respiratory chain turnover in vivo. *Proceedings of the National Academy of Sciences*. http://doi.org/10.1073/pnas.1221132110

Wang, C.-W., & Klionsky, D. J. (2003). The molecular mechanism of autophagy. *Molecular Medicine (Cambridge, Mass.)*, *9*(3-4), 65–76.

Witt, M., Bormann, K., Gudziol, V., Pehlke, K., Barth, K., Minovi, A., et al. (2009). Biopsies of olfactory epithelium in patients with Parkinson's disease. *Movement Disorders*, *24*(6), 906–914. http://doi.org/10.1002/mds.22464

Wong, S. L., Gilmore, H., & Ramage-Morin, P. L. (2014). Parkinson's disease: Prevalence, diagnosis and impact. *Health Reports - Statistics Canada*, *25*(11), 10–14.

Xie, Z., & Klionsky, D. J. (2007). Autophagosome formation: Core machinery and adaptations. *Nature Cell Biology*, *9*(10), 1102–1109. http://doi.org/10.1038/ncb1007-1102

Yahr, M. D., Duvoisin, R. C., Schear, M. J., Barrett, R. E., & Hoehn, M. M. (1969). Treatment of parkinsonism with levodopa. *Archives of Neurology*, *21*(4), 343–354.

Yang, Q., She, H., Gearing, M., Colla, E., Lee, M., Shacka, J. J., & Mao, Z. (2009). Regulation of neuronal survival factor MEF2D by chaperone-mediated autophagy. *Science (New York, N.Y.)*, *323*(5910), 124–127. http://doi.org/10.1126/science.1166088

Youle, R. J., & Narendra, D. P. (2010). Mechanisms of mitophagy. *Nature Reviews. Molecular Cell Biology*, *12*(1), 9–14. http://doi.org/doi:10.1038/nrm3028